Internal combustion engines powered by syngas: A review

Matilde Fiore [1,2], Vinicio Magi [1,3,*], Annarita Viggiano [1]

[1] School of Engineering, University of Basilicata, Potenza 85100, Italy

matilde.fiore@unibas.it

annarita.viggiano@unibas.it, ORCID: 0000-0002-7874-6377

vinicio.magi@unibas.it, ORCID: 0000-0003-1724-2121

[2] Von Karman Institute for Fluid Dynamics, Sint-Genesius-Rode 1640, Belgium

[3] Department of Mechanical Engineering, San Diego State University, San Diego, CA 92182, USA

[*] Correspondence: vinicio.magi@unibas.it

ACCEPTED MANUSCRIPT

Cite as: M. Fiore, V. Magi, A. Viggiano, Internal combustion engines powered by syngas: a review, Appl. Energy 276 (2020) 115415. https://doi.org/10.1016/j.apenergy.2020.115415

© 2024. This manuscript version is made available under the CC-BY-NC-ND 4.0 license https://creativecommons.org/licenses/by-nc-nd/4.0/

Internal Combustion Engines Powered by Syngas: a Review

M. Fiore[1,2], V. Magi[1,3], and A. Viggiano[1]

[1] *School of Engineering, University of Basilicata, Potenza 85100, Italy*
[2] *Von Karman Institute of Fluid Dynamics, Sint-Genesius-Rode 1640, Belgium*
[3] *Department of Mechanical Engineering, San Diego State University, CA, USA*

June 7, 2020

Abstract

Syngas is an intermediate step towards the transition from carbon-based to hydrogen-based fuels, promoted by the emerging concerns about climate change and damages to the environment. The negative impact of power generation systems will surely increase due to the continuous rise in energy demand. As a result, alternative methods must be found to reduce stationary and transport engines energy consumption and pollutant emissions, and the use of syngas as a fuel could be a very promising solution. This review is an attempt to aim and promote a wider employment of syngas as a fuel for internal combustion engines. Hence, after an overview of the technologies for syngas production, a detailed analysis of different applications of this gaseous fuel is presented and discussed. Specifically, dual-fuel Compression Ignition engines, Homogeneous Charge Spark Ignition engines and Direct Injection Spark Ignition engines have been investigated under syngas operating conditions from both experimental and numerical points of views. The performance and the emissions of such engines are carefully analysed and discussed. Indeed, they are very sensitive to the physical and chemical properties of syngas, i.e. the amount of CO and H_2, the laminar flame speed, the wide range of flammability and the lower density of syngas compared to air density.

Keywords: Syngas, gasification, combustion, ICEs, emissions

Introduction

The interest in the use of syngas in internal combustion engines began in India [1, 2, 3, 4], due to its richness of bio-resources and its shortage of fossil fuels, although producer gas had been already used during the World War II to feed power and heat generation systems [5]. The use of residual of forest activities or wastes from agrifood industry is particularly beneficial in small plants where stationary engines are employed for power and heat generation, in order to supply energy to peripheral areas with minimum pollutant emissions. The employment of syngas could strengthen the framework of the circular self-sustaining economy, and if results of research indicate feasibility, syngas could be also used in other applications, such as in the automotive industry.

Syngas production technology

Syngas is produced through the gasification of coal, biomass or wastes into a high temperature environment. The controlled operating conditions and the oxygen deficiency induce a partial oxidation of the feedstock producing a gaseous fuel which is called syngas.
Gasification consists of a sequence of five processes that occur inside a gasifier. Figure 1 shows the sequence of such processes. *Drying* occurs below 100°C and is aimed at eliminating the feedstock moisture content to obtain a very clean gas at the outlet. The dry matter is exposed to heat during *pyrolysis*, when heavy volatile compounds (tars) are vaporised until the biomass reaches a temperature of about 240°C. Tars are composed of more complex molecules than hydrogen and carbon monoxide. Besides tar gases, the result of this process is a solid carbonaceous material known as charcoal which is constituted by fixed carbon-to-carbon chains. *Combustion* is the only exothermic stage among these five processes and its heat release has to support the whole gasification process. Water and carbon dioxide as products of several oxidation reactions are formed during this stage. *Cracking*, immediately after the carbonaceous particles combustion, is needed to turn tar compounds into simpler molecules by the exposure to heat.

Molecular breakdown is essential to yield a gas that should be compatible with an internal combustion engine, as tars could condense into sticky tars which may damage the engine valves. Finally, *reduction* is the process that ensures the formation of hydrogen and carbon monoxide starting from water and carbon dioxide. Reduction is performed by flowing the combustion products across a bed of red hot charcoal, to obtain a high fraction of fuel gas at the outlet.
Gasifiers layout (Figure 2) noticeably affect syngas quality and its chemical composition. Fixed bed gasifiers can be employed, where the gasification of coal or biomass is achieved by passing the feedstock into one or two stages. *Downdraft* gasifiers are characterized by opposite fluid flows and higher temperatures which lead to higher heat losses and low efficiencies. Oxider and fuel flows follow the same path into *updraft* gasifiers, where the temperatures are quite lower. The syngas flow is directed upward carrying tars with it: as a consequence, tars constitute a non-negligible fraction in the gas produced. Operating temperatures can be further reduced with the use of moving bed gasifiers, which usually lead also to an increase of the gasification system efficiency. We move from a *bubbling bed* gasifier (BFB) to a *circulating bed* gasifier and finally to a *transport bed* gasifier as the gas speed increases, gradually achieving better efficiencies and carbon conversion levels. The main advantage of bubbling bed gasifiers is their significant tolerance regarding the feedstock quality, thanks to their blending capabilities and the thermal inertia of the bed particles. In circulating fluidized bed, particles residence time is very long and this technology is then recommended for fuels containing a high fraction of volatile compounds. A wide variety of feedstocks can be used instead in *rotary klins* reactors. The main drawback of this technology is that the complete oxidation of the fuel is difficult to avoid at the inlet where hot spots are easily produced. The feedstock is put on a grate in *moving grate* reactors, and the oxider flow is addressed above and below it. This kind of gasifiers is very tolerant to chemical and physical variations of the fuel and provides a high residence time of the feedstock particles. *Plasma reactors* are the most expensive ones for biomass or coal gasification: they can achieve very high temperatures (2700°C-4500°C) which are able to promote tar cracking and elimination of toxic compounds.

Usually, fuel energy is partially contained in tars, which condense at relatively low temperatures and have to be removed to avoid the engine damage. However, filtration of tar compounds often represents almost one third of the overall investment and leads to several issues of maintenance. The dust content requires a frequent flushing of the filters and a continuous maintenance [1].
Several experimental investigations were carried out to study the effect of the gasifier operating conditions on syngas composition at the outlet and its flow rate with various feedstock types. Depending on the particular syngas application, the gasification process may be addressed to maximize either the hydrogen content [2] or the lower heating value, always ensuring good carbon conversion efficiencies and thermal efficiencies of the process. The influence of the fixed bed temperature and syngas chemical composition was studied by Yan et al. [3] and Nipattummakal et al. [2], in case of biomass char and sewage sludge gasification, respectively. Their results indicate that the higher the temperature, the higher syngas yield is detected, as high temperatures promote the release of volatiles, the endothermic reactions and tar reforming and cracking. For the same reasons, high temperatures also maximise the carbon conversion and the thermal efficiency of the systems. However, the maximum H_2/CO ratios were found at intermediate temperatures, when the water-gas-shift reaction is the dominant reaction of the gasification process, also supported by a proper quantity of steam.

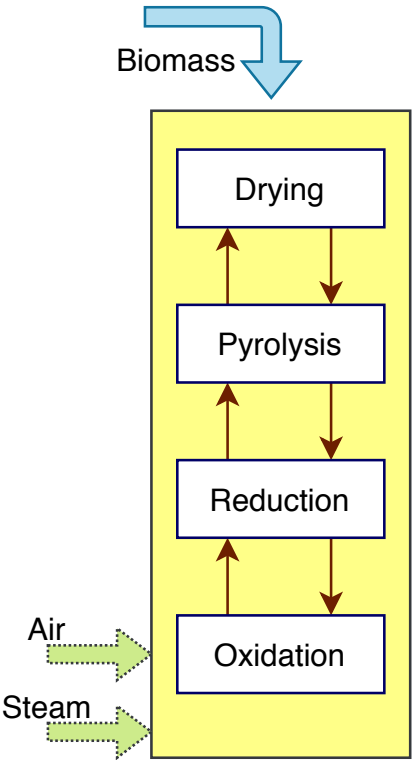

Figure 1: Scheme of the gasification process.

Corresponding Author: vinicio.magi@unibas.it

The need of achieving high H_2/CO ratios and good thermal and carbon conversion efficiencies at the same time led He et al. [4] to investigate the use of a $NiOAl_2O_3$ catalyst for polyethylene gasification, that was able to improve the H_2 contents at high temperatures, as well as the carbon conversion levels, the tar content and the gas yield. Similarly, calcinate dolomite was used in Ref. [5] as a catalyst for Municipal Solid Waste (MSW) gasification, showing comparable benefits in terms of H_2/CO ratios and carbon conversion efficiencies.
The attempt to improve the performance of the gasification systems also involved the analysis of co-gasification processes [6, 7, 8, 9, 10, 11, 12]. For some cases, a synergic interaction between the two feedstocks was detected [6, 8]: for example, Ahmed et al. [6] studied polyethylene and woodchips steam co-gasification, whose good performance suggested a synergy between the compounds. After analysing coal and switchgrass co-gasification, Brown et al. [10] came even to identify the biomass as a kind of inexpensive catalyst for coal gasification.
Given the high investment cost required to set the experimental facilities, the development of predictive models to get syngas composition is utmost important. The models employed to analyse the gasification process could be separated on the basis of their complexity and their computational cost.
The less expensive approach consists of applying equilibrium zero-dimensional models, based on the hypothesis of perfect stirring inside the reactor. The equilibrium of a single global reaction is obtained by imposing conservation of mass and energy and minimizing the Gibbs free energy associated to several main chemical reactions which effectively describe the gasification process. This technique was adopted in the studies of Azzone et al. [13], Altafini et al. [14], Huang et al. [15], Silva and Rouboa [16], Jarungthammachote and Dutta [17], Simone et al. [18] and Ghassami and Shahsavan-Markadeh [19]. The models described in Refs. [13, 14, 15, 16, 17, 18, 19] present some similarities: all of them are based on thermodynamic models that require the thermodynamic properties of the species involved. Such models were able to predict the syngas composition at the outlet in terms of hydrogen, carbon monoxide, methane, water and carbon dioxide mass fractions. A more detailed equilibrium model was proposed by Mountouris et al. [20], who include the calculation of soot beside the main gasification products, and by Barman et al. [21], who estimate tars compounds at the outlet of a downdraft system. Such equilibrium models are easy to use and largely applied to get the syngas composition and are mostly preferred to CFD or heuristic techniques. In fact, detailed CFD models require the definition of complex sub-models whose assumptions are usually difficult to verify. In addition, such models involve the simulation of large computational domains with many geometrical complexities. These approaches are chosen by some authors [22, 23, 24]. Key issues of these works are the mathematical modelling of the two-phase flow (Eulerian-Eulerian or Eulerian-Lagrangian approaches) [23, 24], turbulence [22], devolatilization [22] and combustion [24]. Correlations and empirical sub-models are widely used in this framework to face such level of complexity.

Corresponding Author: vinicio.magi@unibas.it

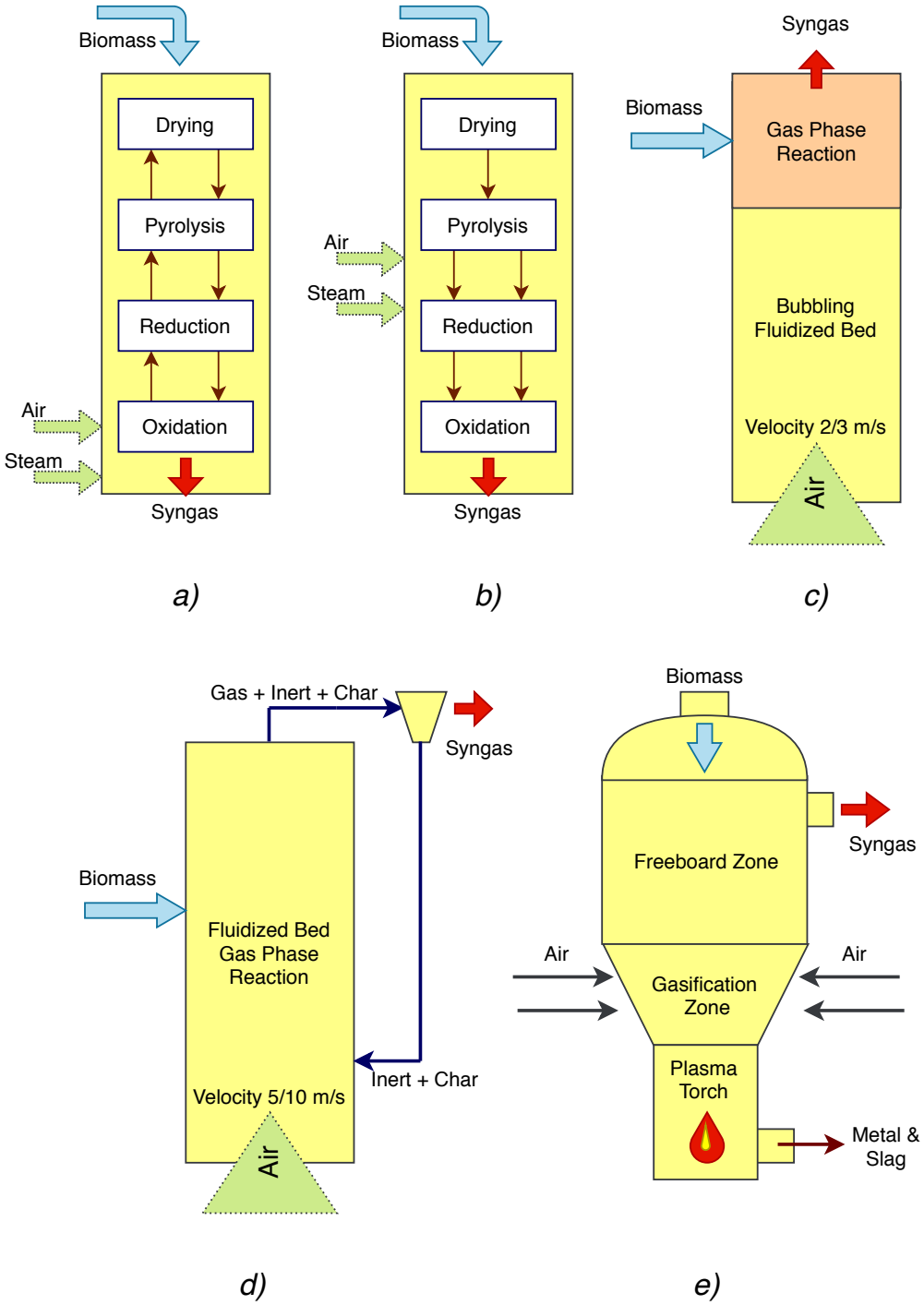

Figure 2: Types of gasifiers: (a) updraft; (b) downdraft; (c) bubbling bed gasifier; (d) circulating bed gasifier; (e) plasma reactors.

Another possibility to model complex gasification processes is represented by Machine Learning techniques, which reduce the system to a black-box connecting input-output data. These tools are aimed at finding regression models for the system, eliminating the need of formulating restrictive assumptions for the chemical and physical phenomena involved. This approach was adopted by Dong et al. [25] and Xiao et al. [26], who developed an Artificial Neural Network to analyse a fluidized bed fuelled with various feedstocks. The main advantage of such approach compared to the numerical ones, is that it does not require a deep knowledge of the involved phenomena to compute system performance with a certain level of reliability. Nevertheless, its spread is limited by the need of a lot of experimental data to perform a good network training.

Corresponding Author: vinicio.magi@unibas.it

Syngas chemical-physical properties and energy content

Syngas consists of hydrogen (H_2), carbon monoxide (CO) and methane (CH_4) as main chemical species, plus eventually a small amount of heavy hydrocarbons. It could contain other species, such as hydrogen sulphide (H_2S), carbonyl sulphide (COS), ammonia (NH_3), hydrogen cyanide (HCN), hydrogen chloride (HCl) and traces of mercury, arsenic and other heavy metals depending on the gasifier feed. The gas is diluted with about 50% of inert gases, such as N_2, H_2O and CO_2, whose volume fractions depend on the gasifying agent used. Different kinds of syngas can be produced (Table 1) depending on the gasifying agent. Syngas derived by the use of steam or oxygen shows a medium heating value of about 10-28 MJ/Nm^3 (simply syngas or powergas), while syngas produced with air is characterized by a lower heating value of 4-7 MJ/Nm^3 and it is generally known as producer gas.
Due to the relatively low calorific value of the producer gas, a drastic reduction of syngas performance compared to conventional fossil fuels is reasonably expected. Actually, this reduction is not that important due to the low air-to-fuel ratio of the syngas-air mixture under stoichiometric conditions. This means that the energy density of the mixture near stoichiometric conditions is almost the same for syngas and for common fossil fuels. The power derating, which occurs with syngas fuelling mode, is attributed only to a partial extent to the lower heating value of the fuel, as it also comes from the decrease of the engine volumetric efficiency [27].
Several properties of the syngas chemical composition make it substantially different from standard fossil fuels. The most important properties are summarized in what follows.

Table 1: Typical syngas and producer gas compositions.

Gas	**Species** (vol %)					
	H_2	**CO**	**CH_4**	**CO_2**	**N_2**	**HC**
Syngas	25-30%	30-60%	0-5%	5-15%	-	-
Producer Gas	13-19%	18-22%	1-5%	9-12%	45-55%	0.2-0.4%

In the first instance, the relatively high laminar flame speed seems to have a significant influence on the engine performance. This is an essential parameter for engine design and pollutant formation, and it is considerably influenced by mixture composition, pressure and temperature. Generally, it is computed based on the H_2/CO ratio of the gas under consideration. A number of works were aimed at determining syngas laminar flame speed as a function of syngas composition, air-to-fuel ratio, in-cylinder pressure and temperature (Kishore [28], Oumette and Seers [29], Liu et al. [30], Fossum and Beyer [31], Natarajan and Seitzmann [32], Monteiro et al. [33], Ai et al. [34], Ravi et al. [35]). Figure 3 shows the laminar flame speed estimated by Kishore [28], as a function of the H_2 and CO volume fractions and the equivalence ratio at 1 bar and 300 K, without CH_4 content. It can be seen that the laminar flame speed increases with the H_2 fraction and that the maximum flame speed is achieved for rich mixtures (ϕ=1.4-1.6). The value of ϕ corresponding to the maximum flame speed reduces as the H_2 fraction increases. As 12% of methane replaces the same fraction of CO (Figure 4), the increase of the laminar flame speed with the hydrogen content is less effective. In Figure 4, the peaks of the flame speed occur at lower values of ϕ compared to Figure 3. The decrease of the laminar flame speed with the equivalence ratio is steeper in the presence of CH_4, which reduces the flammability range.
Beside methane, the fuel inert content tends to considerably reduce the laminar flame speed of syngas-air mixtures. Preferential diffusion of hydrogen and non-unitary Lewis number effects generate flame instabilities [28]. Thermal diffusion (Soret effect) is not negligible: variations higher than 5% of the effective burning rate were calculated even with 5% of hydrogen [28]. Measurements at various Karlovitz numbers indicated a weak dependence on the flame stretch [33]. Difficulties in predicting the actual flame speed essentially derives from the wide variability of syngas composition, which results from a number of factors related to its production technology.

Corresponding Author: vinicio.magi@unibas.it

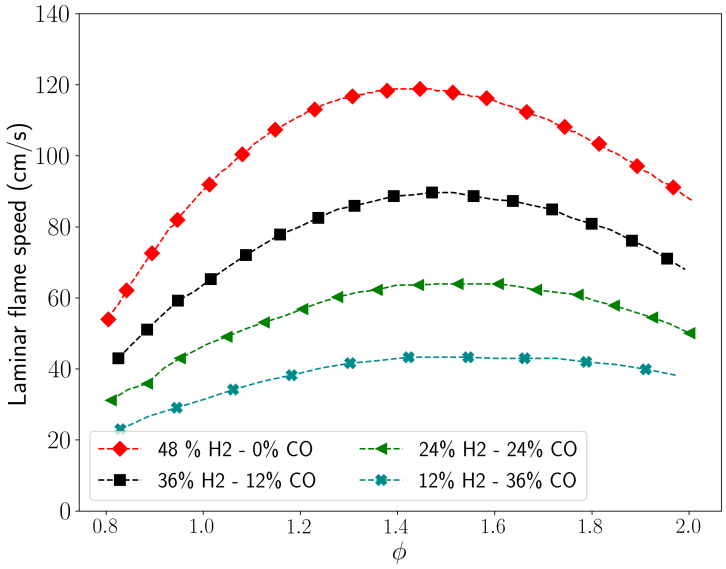

Figure 3: Syngas laminar flame speed as a function of the equivalence ratio with different chemical composition [28] (0% CH_4).

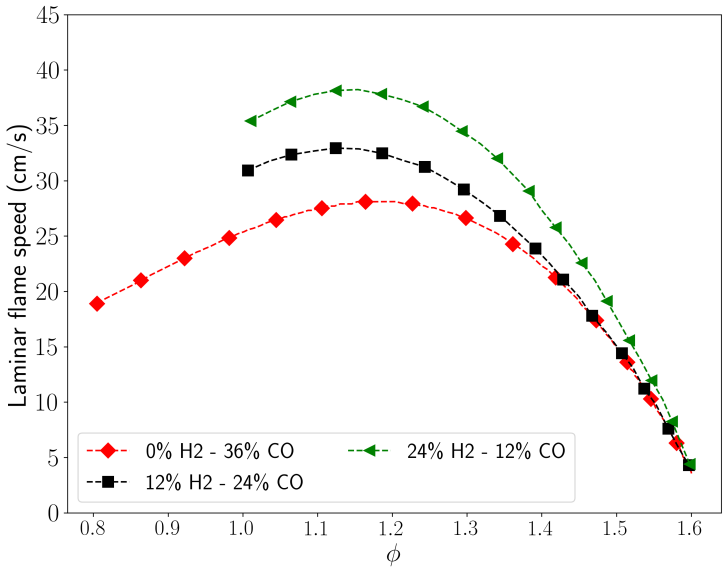

Figure 4: Syngas laminar flame speed as a function of the equivalence ratio with different chemical composition [28] (12% CH_4).

Another important syngas property is its wide range of flammability. This is particularly useful for engine applications as it allows to use this gas even far from stoichiometric conditions. Kutcha [36] and Fossum and Bayer [31] studied the flammability limit as a function of pressure, concentrations and temperature. They found an operating range of 20-60% fuel in air and highlighted the wider range of flammability of syngas compared to natural gas and gasoline. Li et al. [37] measured the lean flammability limits of syngas-air mixtures in a counterflow diffusion flame structure at different levels of inert dilution and unburnt gas preheating temperatures. Such limits seemed to be unaffected by the inert content (N_2 and CO_2) up to a certain level of dilution, even though this critical content decreases when carbon dioxide is the dominant diluent. The effect of inert dilution was also analysed in [18] with the application of the Le Chatelier's Rule. The authors concluded that the lean flammability limit is more affected by the inert content than by the unburnt gas temperature. Shih et al. [38] determined the flammability

Corresponding Author: vinicio.magi@unibas.it

limits of opposite jets of syngas/air assuming an axisymmetric counterflow diffusion flame. The ignition map, derived from the application of a radiation model and detailed chemical kinetics, provided the flammability zones as a function of the strain rate, hydrogen, oxygen and diluents amounts. Turbulence and radiative heat losses seemed to be the main causes of quenching and flame blow-off occurring at high and low strain rates, respectively. These characteristics are very important to predict potential performance, safety and emissions composition.

Several mechanisms were developed to model the chemical kinetics of this gaseous fuel (Table 2). In most of the cases, these reduced mechanisms were derived from detailed ones (e.g. GRI-Mech mechanisms [39]) by reduction techniques, like sensitivity analysis and principal component analysis, or by a merging of the sub-mechanisms of H_2 and CO, which are essential for all mechanisms that involve complex hydrocarbon molecules. The result of such a reduction is a skeletal mechanism with a reduced number of species and reactions, which is valid for a given range of pressures, temperatures and equivalence ratios. Sensitivity analysis [40] shows that hydrogen plays the main role to control the reactivity of the mixture, while CO has an inhibiting effect on chemistry, as it increases the ignition delay time by a factor of 2 with the introduction of 50% of CO, and by a fraction of 10 with a concentration of 90%. Indeed, mixture reactivity is highly affected by the rates of production and destruction of OH radicals. As syngas contains other species beside H_2 and CO, efforts were made to extend the range of applicability of the mechanisms to more reactants and diluents, as methane, carbon dioxide and vapour [41].

The kinetic mechanisms often support the numerical models to simulate syngas power systems and, as such, they have to be accurate as regard chemical reaction rates and pollutant formation. Indeed, most of the mechanisms include additional reactions to represent the interaction of the species with nitrogen [40] to correctly estimate the production of NO_x. Some of the mechanisms given in Table 2 were applied by Maurya et al. [42] to simulate a HCCI engine fuelled by syngas for different values of the intake temperature. The comparison among those mechanisms (Figure 5) show the supremacy of the GRI 3.0 mechanism. Such an approach is highly recommended for engine simulations, although a sensitivity analysis of the kinetic mechanism is generally not carried out.

Table 2: Chemical kinetics mechanisms for syngas combustion.

Ref.	**Num. chemical**		**Range**		**Equivalence**	**Validation**
	spp.*	**rxn.†**	**p** [atm]	**T**[K]	**Ratio**	**data**
Keromnés et al.[40]	14	41	0.987-69.085	914-2220	0.1-4.0	[43, 44, 45]
Frassoldati et al.[46]	12	32	0.039-450	298-2850	0.0005-11.6	[47, 48, 49]
Nikolaou et al.[41]	8	5	1-20	298-700	0.4-5.0	[50, 51, 52]
Davis et al. [53]	14	30	0.047-64	298.2-2625	0.84-3.0	[54, 55, 56]
Petersen et al. [57]	38	190	40-260	1040-1500	0.2-6.0	[57, 58]
Saxena and Williams [59]	13	30	1	298	0.6-4.5	[60, 61, 62]
Sun et al. [63]	15	33	1-40	298	0.3-5.0	[64, 65, 66]
Li et al. [66]	20	84	0.03-9.6	300-2850	0.005-6.1	[67, 44, 62]
Starik et al. [68]	15	44	0.01-60	850-2900	0.3-5.0	[69, 70, 71, 72, 53]
Yetter et al.[47]	13	28	0.3-2.2	823-2870	0.0005-6.0	[44, 73, 74]
GRI mech.3.0 [39]	53	327	0.033-19.7	300-2800	0.0005-6.0	[44, 73, 74]

* species †reactions

Corresponding Author: vinicio.magi@unibas.it

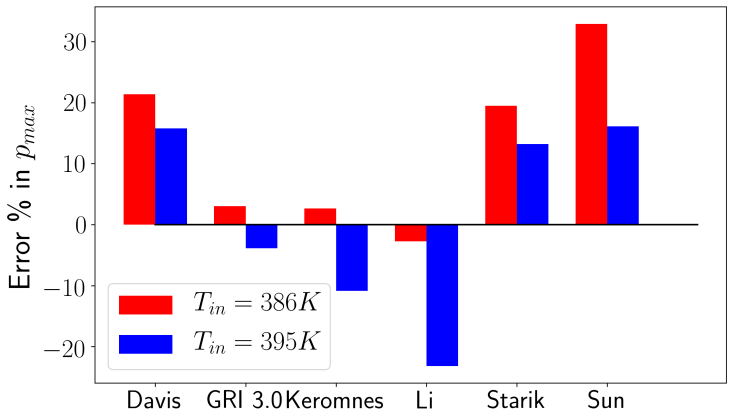

Figure 5: Error in the computed maximum in-cylinder pressure of a syngas HCCI engine ($\phi = 0.3$) with different kinetic mechanisms [42].

Emissions and EGR benefits

The use of syngas in engines may lead to advantages in terms of exhaust emissions if the engine operating conditions are carefully selected. Indeed, pollutant emissions as sulphur compounds, metals, halogens and fly ashes are generally avoided thanks to the cleaning systems that are able to remove the contaminants before being burnt in engines or gas turbines. As a consequence, the most important emissions are limited to NO_x and CO. The amount of CO is also related to the specific syngas composition and its CO content, whereas NO_x is related to the engine geometry and its operating parameters for a larger extent. The significant emission of NO_x is a result of the high flame speed and combustion temperature, and may bring to negative consequences on the performance of the engine. One of the most promising strategies to reduce NO_x emissions near stoichiometric conditions is the exhaust gas recirculation (EGR), which is able to generate a low-NO_x combustion [75]. The EGR technique involves the recirculation of a portion of exhaust gases (mixture of water, carbon dioxide and nitrogen) back into the engine cylinder chamber, to achieve a decrease of the peak temperature.
However, the benefits of the EGR strategy in the context of syngas combustion seem to go beyond the mitigation of pollutant emissions. EGR has a stabilising effect on the flame propagation, as it tends to increase the flame thickness and reduce its resistance to the hydrodynamic perturbations related to the thermal expansion. EGR stability implications were also investigated by Vien [76] with the use of spherical and cylindrical chambers with a Schieleren/shadowgraph setup. Exhaust gas concentrations acted as an energy sink, reducing the flame speed and the adiabatic temperature and delaying the formation of unstable cellular structures. The same damping effect of exhaust gases was discussed by Badhuri et al. [77], who evaluated thermal and kinetic effects of the EGR technique and its influence on the combustion process. The slower combustion arising from exhaust gas dilution gave a significant improvement of the IMEP (25 %) and reduced the engine wall temperature.
EGR is also able to avoid irregular combustion and reduce the knock risk [78], although syngas has a high knock resistance and it does not generally need anti-knock strategies for typical engine compression ratios. This justifies the concurrent use of EGR and syngas blending as major tools to mitigate knock risk with standard fossil fuels [79].
The EGR was also employed in [77] as a strategy to efficiently operate at higher intake temperatures than the tar dew point, thus eliminating the need of a tar filtration system. Indeed, high intake temperatures increase the knock risk and impose more restrictions on the maximum equivalence ratio to be used. In a more recent work of Badhuri et al. [80], the EGR dilution was used to extend the maximum ϕ and mitigate the power derating occurring with syngas at high intake temperatures. The experiments were still preliminary as a simulated exhaust gas composition (mixture of N_2, CO_2 and H_2O) was employed for the experimental campaign. Nevertheless, this approach seems very interesting to reduce filtration costs, and further analysis are recommended to clarify the effective economical gain of this solution.

Corresponding Author: vinicio.magi@unibas.it

Syngas applications and development of specified solutions

Syngas can be employed in internal combustion engines in different ways. As an example, it can be successfully used in Compression Ignition (CI) engines, where higher compression ratios, usually higher than 14:1 and often exceeding 22:1, ensure good thermal efficiencies. As syngas autoignition is difficult to be achieved, diesel fuel is then used as a pilot fuel to ignite the charge. In the case of dual fuel engines, the challenge is to substitute the highest amount of diesel fuel with syngas to ensure good performance and low emissions at the same time. In this context, the outcome can be widely different. Indeed, significant diesel replacements from 30% to 90% are given in the literature, with levels of power derating depending on the syngas composition and on the specific combustion regime, which in turn is a consequence of the injection timing.
Syngas fuel is also employed in Homogeneous Charge Spark-Ignition (HCSI) engines where it replaces gasoline or natural gas. A reduction of the engine performance generally occurs under standard engine operating conditions. One of the common strategies is to increase the compression ratio to achieve engine performance comparable to those obtained with conventional fossil fuels. This is allowed by the reduced knocking tendency of syngas. However, some authors [81, 82] claim that the decrease of the engine volumetric efficiency is the main reason of the lower output power under syngas fuelling mode. This parameter definitively reduces after switching to syngas fuelling mode due to the high air-to-fuel ratio and the low syngas density. This drawback could be overcome by means of direct injection of syngas in the combustion chamber or by employing supercharged engines.
Specific arrangements are required to handle such a gas in ICEs, as most of the engines were originally designed to operate with gasoline, diesel fuel or natural gas. Clearly, a certain variability of syngas composition can only exacerbate this problem, and enhances the need of prevention systems and appropriate regulation devices.
Specific features of these engines may consist on flame arrest to prevent backfire, given the large reactivity of hydrogen and the wider combustion intervals of the other main species, such as methane and carbon monoxide, which could keep burning even after the exhaust valve opening. For such purpose, General Electric developed the Jenbacher Gas Engine [83], which was designed to run with very lean syngas-air mixtures and avoid troubles as pre-ignition, knocking or engine backfire. The engine also offers a better accessibility to the exhaust gas manifolds, thus favouring cleaning and maintenance.
Other researchers try to build up specific carburettors using experimental [84] or numerical approaches [85, 86, 87, 88, 89, 90]. These investigations were aimed at obtaining a good mixing of air and syngas under the entire load range, avoiding high pressure losses. The carburettors should be also easy to regulate, and problems of hysteresis have to be minimized to ensure reproducibility [84]. Different configurations were analyzed to achieve these goals [88, 90], also based on the resulting performance of the engine and its emissions [90].

Economical Aspects

Recovery strategies based on syngas gasification and combustion in ICEs are generally based on small-scale plants. Indeed, the profitability of such systems strongly depends on the local availability of appropriate wastes and feedstocks, whose transportation is generally not affordable. Obviously, this requirement holds down the possible earnings, preventing scale effects to be fully exploitable. Such scale effects are important [91] and Figure 6 shows how the cost of the syngas production reduces more than linearly with the increase of the power capacity.
Since large plants are not feasible in this context, the profitability of small local systems was analysed by the authors [92, 91, 93]. Their configurations included electricity, syngas [91] and hot water production [93], as well as cold water production from absorption refrigerators [92]. The analyses consider maintenance, operation and investment costs for all the components of the system, i.e. gasifiers, heat exchangers, refrigerators, engines, etc. For these plants [91, 92], the estimated payback period was 4-5 years with the assumption of 3000 working hour/year. This can be seen in Figure 7, where the annual expected saving obtained in [93] is shown as a function of time and of the load of the generation system. For a payback period ranging from 2 to 7 years, the system should operate for a minimum of 2000 h/year to be competitive.

Corresponding Author: vinicio.magi@unibas.it

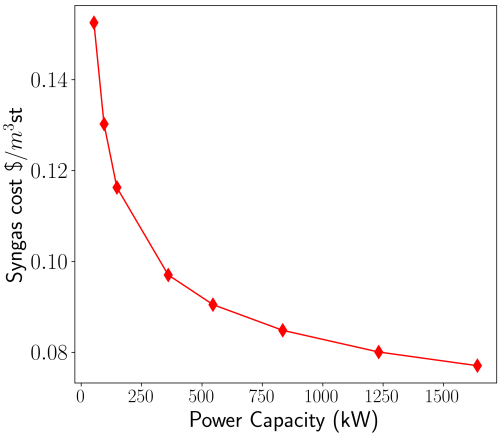

Figure 6: Decrease of the syngas cost with the increase of the plant size [91].

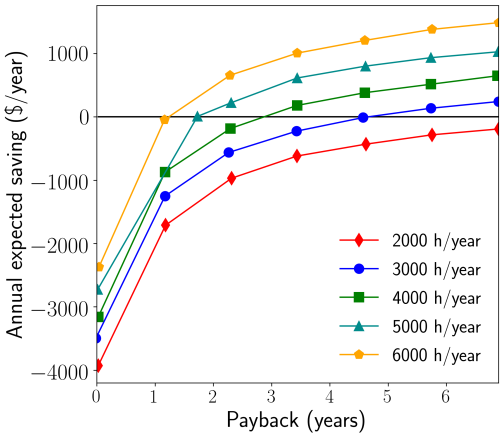

Figure 7: Annual saving for different annual working hours [93].

In Ref. [93], the electricity production cost resulted lower than the electricity fare, though this was not for the generated hot water, which was instead more expensive. The estimated hot water cost is lower in Ref.[92], where water is heated by both the exhaust gases and the gas exiting from the gasifier. The layout of the system is indeed very important for such recovery systems. As a matter of fact, the gas enthalpies are lower compared to other applications and all the energy recovery sources must be used to end up with optimal efficiencies.
In Ref. [91] the use of dual fuel and spark ignition engines were compared from an economic point of view. The spark ignition technology was characterised by higher investment costs compared to dual fuel engines, since the capital costs were also related to the level of development of both technologies. Conversely, higher operational costs characterised the dual fuel technology. The use of spark ignition engines provided positive values of NPV for power capacities ranging from 60 to 1640 kW.
Such analyses assessed that the use of syngas is economically competitive. This is likely to become even more important in the near future, due to the rising cost of petroleum-based fuels. The filtration and cleaning costs associated with syngas production will also decrease, if specific strategies will be able to increase the tolerability of the engines with respect to the syngas chemical composition (e.g. the use of EGR to increase the intake temperature without reducing the performance). In addition, the worldwide progress of recycling practices would facilitate the retrieval of good feedstock, thus allowing an increase of the size of these plants and the use of scale economics.

Structure of the Work

This work is an attempt to provide an extensive review of a large variety of applications of syngas in internal combustion engines and to show all the fundamental issues related to its use. Important findings accomplished over the years are reported in this work with reference to specific operating fields. The work consists of separate sections, each of them addressed to the use of syngas for specific engines. In Section 2, the use of syngas as a dual-fuel for compression ignition engines is described. Section 3 is focused on the use of syngas for homogeneous charge spark-ignition engines, and presents the main outcomes in terms of emissions, efficiency and brake power output. Then, numerical and experimental analysis on the use of syngas in Direct Injection Spark Ignition (DISI) engines are presented in Section 4. Concluding remarks are finally given and a comprehensive list of references is provided for the reader.

1 Syngas as a fuel for Dual-Fuel CI engines

In dual-fuel CI engines, the heat released by combustion comes in part from diesel fuel, and in part from an alternative fuel, e.g. syngas. The dual-fuel mode is aimed at minimizing the consumption of diesel fuel on the basis of environmental and/or consumption considerations. To this end, the optimal amount of diesel fuel to be employed needs to be determined over the whole range of the engine operating conditions, in order to reduce specific fuel consumptions and obtain the best performance at various

Corresponding Author: vinicio.magi@unibas.it

engine loads. The literature provides considerable materials on the success of such a technology from economical and environmental perspectives. A decrease of power output in dual-fuel mode is stated in most of the available works. This decay is due to the reduction of the gas heating value in the case of producer gas and to the drop of the volumetric efficiency in the case of syngas. A net reduction of emissions, mainly CO and HC, was observed under medium load conditions, whereas new strategies were required to control NO_x. A specific regime of combustion (PREMIER combustion) was observed during the experiments. This regime results from the superimposition of more stages of heat release, and it seems to be very favourable in terms of engine performance. Further improvements in terms of combustion control were obtained with the use of Reactivity Controlled Compression Ignition (RCCI) engines, which involve an early injection of a pilot fuel during the compression stroke.
Advanced numerical models were developed to simulate the working cycle of these engines, and optimization algorithms were successfully integrated into CFD codes to properly set several engine parameters. Higher accuracy of numerical simulations could be achieved by improving turbulence/chemistry interaction models and by optimizing geometrical parameters related to injectors, combustion chambers and intake/exhaust pipes. The integration of feedback control techniques into numerical codes would be able to reduce the number of simulations of genetic algorithms to get the optimal solutions. Nowadays, this is the main issue that prevents the numerical approach to be always convenient. Hence, this is one of the path to be followed for future studies in this field.

1.1 Diesel fuel savings

First investigations on the use of syngas in ICEs under dual-fuel mode were carried out in ‘80s. These experimental studies were addressed to verify whether diesel fuel could be substituted by syngas. Dennetiere et al. [94] and Vyarawalla et al. [95] studied gasifier-engine systems operating with biomass converted in producer gas. Vyarawalla et al. [95] stated that the downdraft gasifier under consideration was capable to operate steadily and reliably to provide a producer gas with an acceptable lower heating value and tar content. This study revealed the possibility of achieving diesel fuel saving of 75-80%. Based on the findings of Dennetiere et al. [94], the use of producer gas derived from agricultural waste is possible and advantageous to guarantee a significant diesel fuel replacement. A more detailed study of Parikh et al. [96] identified some parameters that considerably influenced dual fuel performance, such that conclusions achieved by various authors are inconsistent for some cases. In particular, the volume of the gas cooling-cleaning system, the turbulence level and the nature of the flow through the gasifier were key factors. In addition, they show that direct injection (DI) and indirect injection (IDI) diesel engines coupled to a gasifier had a good impact on the quality of the gas produced. Production of tar and particulate remained a matter of concern and the gasifier took a certain time to produce a stable outflow. The direct injection and the indirect injection diesel engines achieved savings of diesel fuel of 80% and 90%, respectively.
The use of dual fuel in engines was analysed in the following years. Sombatwong et al. [97] carried out engine tests to evaluate the performance of a diesel, four strokes, naturally aspirated engine operating under dual-fuel mode. Diesel fuel and producer gas were used in the experiments and performances were evaluated varying the load and the pilot fuel flow rate. The use of producer gas allowed a certain level of diesel saving, which achieved a maximum value of 64.21%, with a diesel mass flow rate of 0.22 kg/s. The diesel saving started decreasing for higher rates of the pilot fuel since the mixture became too rich. Diesel fuel replacement cannot exceed a certain level as the engine thermal efficiency tends to decrease with the amount of gaseous fuel. Indeed, engine efficiency improves as the amount of diesel fuel increases. A number of ignition spots take place during the injection, leading to a higher energy released during charge ignition that promotes flame propagation and heat release rate during premixed combustion. Hence, difficulties arise to simultaneously control engine efficiency and diesel fuel consumptions , due to the unfavourable correlation between them. Mahgoub et al. [98] used three different syngas compositions (A, B and C in Table 4) and found the highest efficiencies (29-37.5%) and power outputs without diesel replacement, regardless of the syngas composition.
Table 3 shows the maximum diesel saving reached by several authors. A diesel saving up to 50% was achieved by Mahgoub et. al. [98] with composition B at 1200 rpm. The maximum diesel replacement of 74.2% at 1200 rpm was obtained with Syngas C, which was also the most favourable gas in terms of efficiency (37.5%) and power output. A similar diesel fuel saving of around 75% was obtained by Dasappa and Sridhar [84], who analysed a diesel-syngas dual-fuel engine which had to meet specific power requirements. However, the efficiency of the engine decreased from 28% to 22% in dual-fuel mode. Uma et al. [99] obtained diesel replacements ranging from 67% to 86% and a considerable increase of

Corresponding Author: vinicio.magi@unibas.it

the specific fuel consumptions. Singh and Mohapatra [51] operated with a CI dual fuel engine fuelled by producer gas and diesel fuel. They measured the maximum diesel fuel reduction of 45.7% at low loads. Malik [1], employed a test-bench including a gasifier and a CI engine optimized to achieve the maximum replacement of diesel fuel, which amounted to 50%.
All those works showed that the dual fuel mode can be usefully employed in order to face the shortage of conventional fossil fuels. Nevertheless, such studies also found a certain power derating (see Figure 8) and a significant increases of specific fuels consumptions (Figure 9), which increased, as an example, from 450 g/kWh to 2000 g/kWh with the use of Syngas A [98]. Moreover, due to the low density of syngas, its storage will become even more troublesome and expensive. This is definitely a key issue of this technology that up to now has restricted the current applications to stationary engines.

Table 3: Maximum diesel saving with dual fuel engines.

Authors and Ref.	**Eng Speed (rpm)**	**Cyl***	**Vol. Dis**	**Max. Load**	**Compr. Ratio**	**Max. Diesel Saving**
Parikh et al.[94]	649.8	1	1428	4.4	22:1	90%
Sombatwong et al.[95]	1500	1	411	5.884	18:1	64.21%
Mahgoub et al.[96]	1200	1	319	4.0	17.6:1	74.2%
Dasappa and Shridar[97]	1800	6	6494	68.4	17.5:1	75%
Uma et al.[98]	1500	6	6614	77	15:1	86%
Singh and Mohapatra[99]	1500	1	553	3.5	18:1	45.7%
Malik [100]	1500	1	553	5.0	18:1	50%

* cylinders

Table 4: Syngas compositions by Mahgoub et al.[98]

Syngas Fuel	**N_2**	**CO_2**	**CO**	**H_2**	**CH_4**	**LHV** [kJ/kg]
A	49	12	25	10	4	4726.19
B	51	6	22	18	3	5418.4
C	38	8	29	19	6	7444.13

Corresponding Author: vinicio.magi@unibas.it

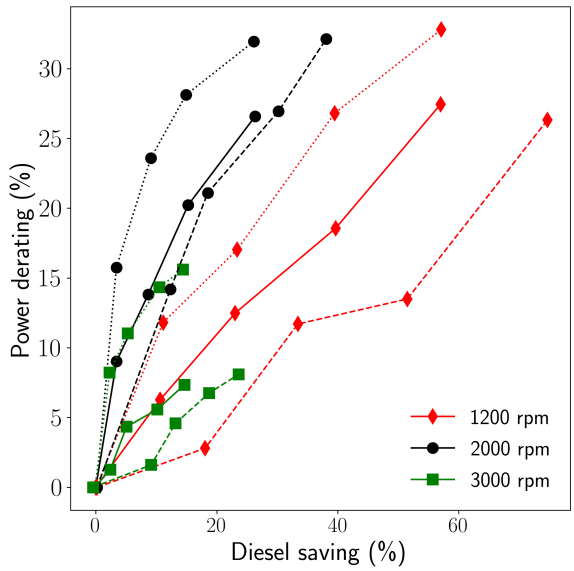

Figure 8: Power derating obtained by Mahgoub et al. [98] with syngas as primary fuel, using compositions A (solid line), B (dotted line), and C (dashed line) of Table 4.

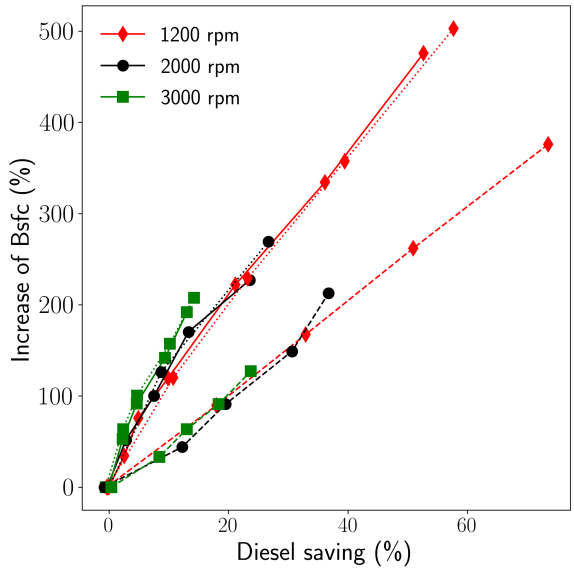

Figure 9: Increase (%) of specific fuel consumptions obtained by Mahgoub et al. [98] with syngas as primary fuel, using compositions A (solid line), B (dotted line), and C (dashed line) of Table 4.

1.2 Dual fuel combustion analysis

In dual-fuel engines, combustion consists of five fundamental steps [100] as shown in Figure 10. The first phase follows diesel injection and it is characterised by the ignition delay of the pilot fuel (phase AB). In this phase, complex chemical reactions take place, which anticipate the heat release by combustion [1]. Generally, the ignition delay time is higher in dual fuel combustion, as the gaseous fuel fraction

[1]Two models are generally used to estimate the ignition delay in dual fuel engines: the first one is based on an Arrhenius equation, and the second one on the integral formulation by Livengood and Wu [101]. Arrhenius equation provides the ignition delay dependence on pressure, temperature and activation energy. This equation has been improved by various authors (Hardenberg and Hase [102], Hiroyasu [103], Mansour et al. [104], Prakash et al. [105]), to include the influence of cetane number, engine speed and oxygen concentrations. Such modifications improved the estimate of the ignition delay in case of dual-fuel combustion.

Corresponding Author: vinicio.magi@unibas.it

reduces the oxygen concentrations within the spray region. In case of diesel-producer gas combustion, the gaseous fuel is characterised by a high inert content and ignition is even longer due to its slow burning properties [97]. At the end of this phase, the injected pilot fuel (diesel fuel) auto-ignites. Several ignition kernels are generated before combustion. Then, a premixed combustion stage occurs and a certain pressure rise is achieved (phase BC). This pressure rise is related to the combustion of mixture of air and diesel fuel around the ignition point. As the flame moves away from the spray region, diesel combustion becomes diffusive and controlled by the fuel mixing rather than chemical kinetics. Phase CD is characterised by a pressure decrease related to the primary fuel delay period. Thus, in the fourth step, a rapid combustion of the primary fuel leads to a second pressure rise (phase DE). Then, combustion proceeds with the contribution of both fuels during turbulent flame propagation (phase EF). Therefore, the combustion process in dual-fuel engines shows the typical features of compression-ignition (CI) engines and spark-ignition (SI) engines at the same time, i.e. a premixed combustion of diesel fuel followed by its mixing-controlled combustion [106], whose heat release rate is enhanced by the simultaneous premixed combustion of syngas.

The analysis of the combustion process in dual-fuel mode was the main issue of the work of Azimov et al. [107], who observed that conventional diesel combustion can be shifted into a two-stage heat release combustion under certain operating conditions : this combustion mode was investigated in several works [107, 108, 109, 110] and it was named PREmixed Mixture Ignition in End-gas Region (PREMIER) combustion. During the first stage of this combustion regime, the pilot diesel fuel is injected, then it auto-ignites before TDC. Diesel fuel ignition brings turbulent flame propagation in the combustion chamber. When the end-gas region reaches the auto-ignition temperature, a second stage of combustion starts and proceeds with very high heat release rates. This autoignition of the charge occurs well far away from the ignition spots, preventing the onset of pressure oscillations and allowing a controlled combustion. In the work of Azimov et al.[107], the advantages of PREMIER combustion regimes in terms of power and efficiency of the engine are well explained. PREMIER combustion was characterized by two peaks of heat release, the highest occurring several degrees after TDC. This combustion behaviour leads to an increase of the performance of the engine, as shown in Figure 11, where the performance of a syngas dual fuel engine with and without the occurrence of PREMIER combustion are compared.

PREMIER combustion differs to knocking combustion for the size and location of the exothermic regions and also for the less sharp gradients and its time frame. Thus, the operating conditions under PREMIER combustion must be properly set to avoid *spark knock* and *diesel knock* [2]. One of the most important controlling parameters is the SOI (Start of Injection) of the pilot fuel. The effect of SOI timing in case of PREMIER combustion was studied by Roy et al. [110], who performed experiments with two syngas compositions, varying the equivalence ratio (within the range 0.4-0.99) and the injection timing from 23° BTDC to 5° ATDC. The transition from normal combustion to a two-stage combustion was observed with lean mixtures at the optimum ignition timing, which was between 23° BTDC and 4° BTDC for very lean mixtures (ϕ=0.4-0.65), and between 7° BTDC and 3° ATDC for near stochiometric mixtures (ϕ=0.83-0.95) to avoid the knock triggering. In Ref. [110], the use of lean mixtures was a rigorous requirement to reproduce the two-stage combustion mode without damaging the engine. Near stochiometric conditions, combustion became indeed less controllable, and the authors [110] were not able to find an intermediate regime between normal and knocking combustion.

A more controlled combustion can be achieved with the use of RCCI engines [111, 112], that allow for a first early injection of the pilot fuel during the compression stroke. The best operating parameters for this combustion mode are not yet identified. Recent analyses [111] regard the fuel optimization ratio and the injection timings (SOIs) for both injections.

[2] These two irregular combustion modes are related to the detonation of the gaseous fuel and of the pilot fuel, respectively. The first takes place when the autoignition of the end-gas happens with intolerable in-cylinder pressure rises. The second one can be a consequence of a long ignition delay, which leads to an accumulation of the pilot fuel forming a homogeneous mixture that spontaneously burns with a very rapid energy release and a severe pressure rise.

Corresponding Author: vinicio.magi@unibas.it

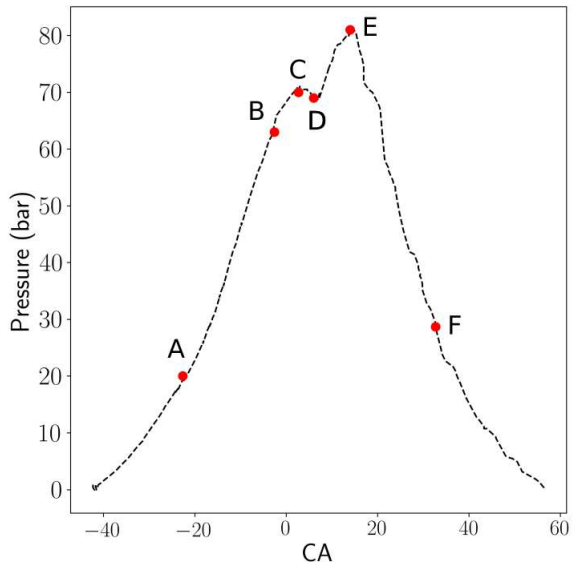

Figure 10: Dual fuel combustion phases (taken from [113]).

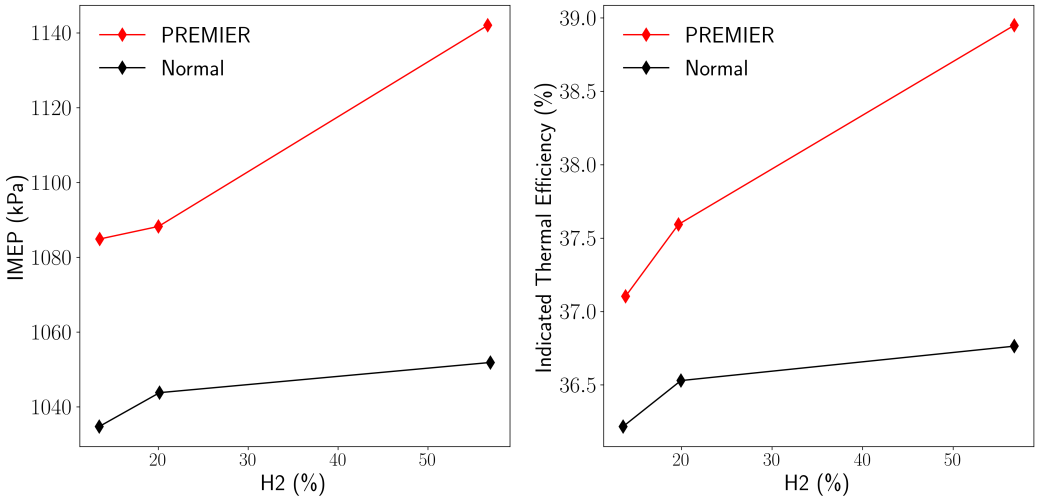

Figure 11: Engine performance with conventional and PREMIER combustion by Azimov et al. [107], as a function of H_2 contents in the primary fuel.

1.3 Volumetric efficiency in dual fuel engines

Several authors [114, 107, 115] tested the dual-fuel mode operation with simply syngas, which consists of a gas almost exclusively composed by hydrogen and carbon monoxide. The sensible reduction of the inert fraction certainly leads to a very different response of the gaseous fuel, and it brings out other specific issues regarding its employment in the engines, e.g. the decrease of the engine volumetric efficiency, as it was underlined by Sahoo et al. [114] and Maghoub et al. [98]. Actually, such an issue seems to be directly linked to the low mass density of syngas compared to air density, and the consequent poor charge efficiency during the intake process. Sahoo et al. [114] measured volumetric efficiencies of 73.7%, 69.5% and 66.2% at maximum load, for H_2 volume fractions of 100%, 75% and 50% in syngas, respectively. Analogously, Mahgoub et al. [98] claimed that the engine volumetric efficiency decreases due to the lower density of syngas compared to air density. The volumetric efficiency significantly varied with the engine speed, and appeared to be slightly affected by the diesel replacement rate (Figure 12).
As expected, a supercharger is able to increase the fuel density and improve volumetric and thermal

Corresponding Author: vinicio.magi@unibas.it

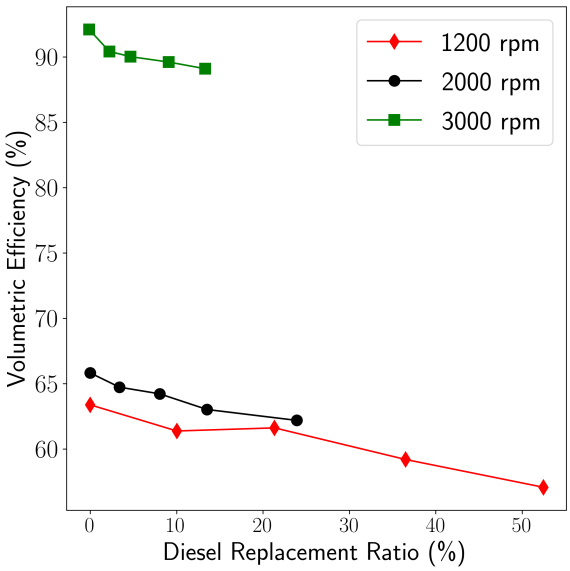

Figure 12: Volumetric efficiency measured by Mahgoub et al. [98] with the use of composition A (Table 4).

efficiencies. Singh and Mohapatra [116] suggested the employment of a supercharged or turbocharged engine for the purpose of reducing the air deficiency under dual fuel mode. Hassan et al. [117] combined the use of a supercharger with higher injection advances. They achieved a remarkable gain in terms of combustion efficiency with respect to conventional premixed dual fuel. As a consequence, CO and CO_2 emissions decreased thanks to the increased oxygen availability which led to an almost complete combustion process.

1.4 Emissions in dual fuel engines

Emissions of nitrogen oxides, carbon monoxide and carbon dioxide are usually measured at the exhaust to assess the dual-fuel engine characteristics in terms of pollutant amounts. Azimov et al. [107] observed an increase of NO_x emissions with the hydrogen content, which contributed to reduce CO and HC emissions on the other side. Similar conclusions were drawn by Roy et. al. [110], who measured CO and HC emissions less than 10-25% with the use of the H_2-rich producer gas, as well as high NO_x emissions. High NO_x emissions at high diesel replacement levels were also found by Boheman and Le Corre [118]. They observed that an early injection of the pilot fuel could reduce maximum in-cylinder temperature and pressure and allow to reach a net reduction of NO_x. In both studies [110, 118], the EGR was viewed as an effective solution to reduce such emission. However, the amount of NO_x emission is probably related to the specific engine operating conditions as well as to the PREMIER combustion mode, which leads to high temperatures and heat release rates during the detonation of the end-gases. Indeed, different results were obtained by other authors. Singh and Mohapatra [116] and Malik [1] experienced a NO_x reduction of 69.5% and 20%, respectively. In particular, the results achieved by Singh and Mohapatra in terms of NO_x are indicated in Figure 13. This net reduction under dual fuel operation is to be expected in one-stage combustion regimes and is indicated also in Ref.[114] and [119], as the temperatures achieved are lower if compared to a standard diesel combustion. Given the advantages of PREMIER combustion, strategies are required to control NO_x. Examples are the use of catalyst reduction, steam or water injection following the injection of the pilot fuel, either a staged combustion in time (multiple diesel injections) or in space (generation of fuel-rich regions separated by air-rich regions).
Other investigations identified CO emission as the most critical one for dual fuel engines [99, 119]. Uma et al. [99] measured pollutant emissions at 80% of the maximum load, concluding that such emissions resulted below Indian standards, except for CO emissions that were higher than those achieved under diesel fuel operating conditions. An increase of CO emissions with the engine load was also indicated by Parikh et al. [96] and Sombatwong et al. [97]. Specifically, Parikh et al. [96] suggested to limit the load in dual fuel mode, as high CO as well as high levels of particulates were detected at high load

Corresponding Author: vinicio.magi@unibas.it

conditions. Conversely, Sombatwong et al. [97] found higher CO emissions in dual-fuel mode over the entire set of operating conditions, as indicated in Figure 14. Such emissions decreased with the amount of pilot fuel since the combustion process improved, thanks to the higher number of ignition kernels and less distance between spots. At high loads, a noticeable concentration of gaseous fuel was achieved in the combustion chamber, thus facilitating the flame propagation. In these conditions, the dependence of carbon monoxide emission on the flow rate of diesel fuel became moderate, as it can be seen by comparing the results of Figure 14 at high values of BMEP. Hence, they stated that the dual-fuel mode was more favourable at high loads[3].

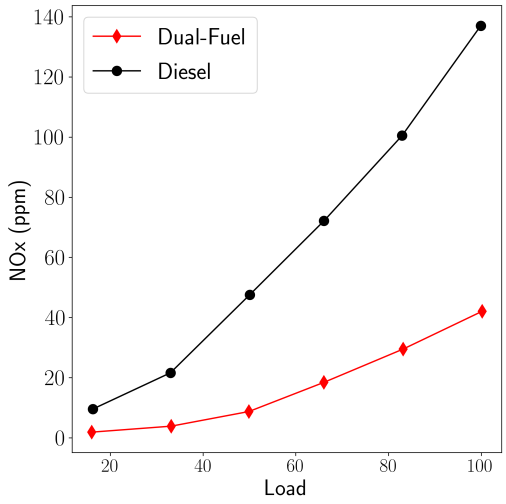

Figure 13: Comparison between NO_x emissions under diesel mode and dual-fuel mode by Singh and Mohapatra [51].

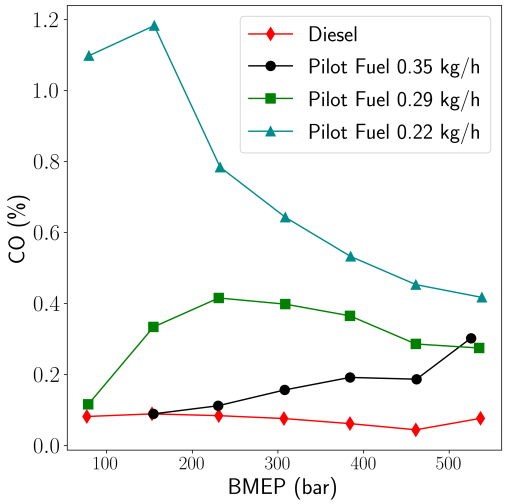

Figure 14: Percentage increase of CO emissions as unburnt CO fuel with the decrease of the amount of diesel fuel (adapted from [97]).

Most of the CO emissions can be drastically reduced by ensuring a complete syngas combustion, which might be more difficult to achieve whether oxygen becomes the limiting agent of the combustion process. Incomplete combustion due to the lack of oxygen was indicated in Refs. [98, 115, 119] as the leading cause of the CO emissions detected in dual fuel engines. Shrivastava et al. [119] measured higher emissions for both CO and HC under dual fuel operation. The lack of oxygen was ascribed to the high intake temperature and low density of the charge filling the cylinder during the intake phase. Higher combustion efficiencies are then needed to mitigate CO emissions in dual-fuel mode. For such purpose, the impact of geometrical parameters as the combustion chamber shape and the injector specifics should be further investigated.

1.5 Fuelling opportunities

Dual-fuel combustion tries to couple the benefits of two fuels with different properties within the same engine. A careful selection of the two fuels is then required to obtain higher thermal efficiency than diesel and spark ignition engines fuelled with standard fuels. This is very much dependent on the compression ratio of the CI engines and on the development of a fast air-gaseous fuel combustion after TDC, which could enhance the heat release rates compared to a diffusive diesel combustion. On a large extent, this combustion regime is dependent on the chemical and physical properties of the fuels.
A wide variety of biomass derived fuels has been examined to set an optimal combination. For example, Ramadhas [120], Malik [1] and Shrivastava et al. [119], Singh and Mohapatra [116] used primary fuels derived from coir pith, cotton stalks and woodchips and oil, sugarcane bagasse and carpentry waste, respectively. Other options were identified for the pilot fuel (Banapuramath et al. [90], Ramadhas et al. [120], Singh et al. [121], Nayak et al. [122], Kashipura et al. [123], Yaliwal et al. [124]).
These investigations are extremely important to design independent and productive energy recovery

[3]At high loads, higher thermal efficiencies were also detected, although the highest diesel fuel saving corresponded to lower efficiencies and higher CO emissions.

systems, which should be related to the vegetal, animal and industrial resources of a given geographical area. Nevertheless, preliminary analysis of such systems are very important to assess their economical and environmental impact and to properly set the operating parameters. For example, Ramadhas et al. [120] used a producer gas derived from coir pith as a primary fuel, whereas rubber seed oil and diesel fuel were selected as pilot fuel. The authors were able to run the engine up to 50%-60% of full load, although they found a higher consumption of rubber seed oil than that of diesel fuel under dual-fuel mode. Unfortunately, CO and CO_2 emissions were higher for producer gas-rubber seed oil than those obtained for producer gas-diesel fuel.
Singh et al. [121] tested a naturally aspirated diesel engine operating with different mixtures of air and diesel fuel, refined rice bran oil and producer gas from a wood gasifier. The work showed that a mixture consisting of 75% of refined rice bran oil and 25% of fossil diesel fuel can be used as pilot fuel after a mixture pre-heating up to 60°C. Producer gas-diesel fuel and producer gas-diesel fuel enriched by refined rice bran oil also led to different outcomes in terms of emissions. Table 5 shows the emissions obtained under diesel operation (FD), rice bran oil-diesel operation (RRBO+FD), producer gas-diesel operation (FD-PG) and mixed operation (producer gas-mixture of refined rice bran oil and diesel fuel). The use of rice bran oil reduced the emissions of HC, though it led to an increase of NO_x. The producer gas composition obtained from the wood gasifier was able to mitigate nitrogen oxides emissions, in both conventional and mixed dual-fuel engines.
Different options were also tested by Nayak et al. [122], who used producer gas from primary fuel and diesel, Jatropa oil[4] and Jatropa methyl ester as injected fuel. The highest thermal efficiency was found under producer gas-diesel fuel operation. Emissions of HC, CO and smoke resulted higher with producer gas-preheated Jatropa oil, whereas the maximum amount of exhaust CO_2 and NO_x were observed with Jatropa methyl ester. Such pollutants were minimum with diesel fuel as pilot fuel.
Obviously, new selections of primary and pilot fuels cannot be adequate for engines specifically developed to run with conventional fuels. However, the results already achieved lead to guess that better settings could improve such new choices in terms of engines performance and emissions. If such improvements were achieved, these energy production systems would not be anymore subject to the transport costs of diesel fuel, becoming even more economically affordable.

Table 5: Emissions detected by Singh et al. [121] in case of conventional and dual fuel combustion with different pilot fuels (84% of full load).

Chemical Species	**FD**	**RRBO+FD**	**FD+PG**	**Mixed Fuel Mode**
HC (%)	0.58	0.47	0.97	0.28
CO_2 (%)	8.06	7.99	6.47	11.3
CO (%)	2.3	0.931	1.04	2.72
NO_2 (ppm)	40.5	51.5	6	7.47
NO (ppm)	1495	1855	249	574

1.6 Dual fuel engine design parameters

Other than engine fuels, also chamber geometry influences the combustion process, as it affects the size and the distribution of the ignition spots, the heat transfer through the cylinder walls and the spatial and the temporal propagation of the flame front. An attempt to explain the effect of the combustion chamber shape on the performance of a dual fuel engines was made by Kashipura et al. [123]. Different combustion chamber shapes were designed to identify their role to control the combustion process and the formation of pollutant agents. Hemispherical (HCC), cylindrical (CCC), trapezoidal (TrCC) and toroidal (TCC) combustion chamber shapes were tested. The study showed that the TCC shape maximized performance and minimized emission levels compared to the other combustion chambers. In particular, the TCC geometry was able to provide an interesting flow structure and a good fuel mixing. An optimization procedure of both the piston bowl shape and the squish area was also done by Ali et al. [125], which was based on the analysis of the combustion process. They found that with a large squish near TDC, the combustion efficiency tends to be less dependent on the chemical composition of the primary fuel.
Kashipura et al. [123] also emphasized the need of optimising the injector geometry and its location to

[4]The Jatropa oil was preheated to reduce its viscosity.

achieve an excellent combination. Yaliwal et al. [124] studied the effect of nozzle type and combustion chamber geometry on performance and emissions of a diesel dual fuel engine running with Honge methyl ester and producer gas as injected and primary fuels, respectively. The increase of the injection pressure and the number of injector holes led to a better fuel mixing and lower pollutant emissions. Although a trade-off between smoke and NOx emissions was observed, the levels of such emissions could be mitigated with the use of a re-entrant combustion chamber configuration, which is schematically shown in Figure 15. The optimized dual fuel engine reached an improvement of thermal efficiency of 5.65 % and reductions of exhaust HC, CO, NO_x and smoke of 11.2%, 17.64%, 15.68% and 19%, respectively. The dual fuel engine operated smoothly, giving good engine performances with a proper choice of both the operating parameters and the chamber specifics.

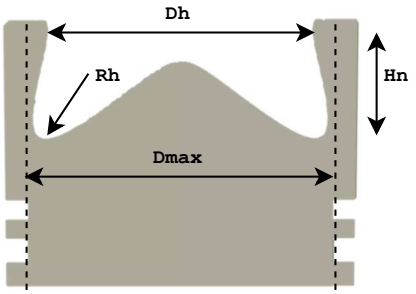

Figure 15: Re-entrant type combustion chamber utilised by Yaliwal et al. [124].

1.7 Numerical modelling of dual fuel engines

Experimental measurements played a fundamental role to clarify the phenomenological aspects of the dual syngas-diesel fuel combustion and identify a large number of parameters that results on engine performances. This was essential to develop predictive approaches based on modelling and numerical simulations. It is well known that the complexity of the combustion process makes difficult to develop numerical or analytical models that comprehensively represent all the involved phenomena. Nevertheless, some modelling efforts were performed, obtaining a good match with the available experimental data.
A simple model based on the application of three Wiebe's functions for the premixed combustion of diesel fuel, the premixed combustion of syngas and the diffusive combustion was developed by Caligiuri and Renzi [126]. This model was addressed to capture the two pressure peaks at the maximum heat release points occurring at different CA. Their approach employed correlations to estimate the heat losses through the cylinder walls (Woschini [127]) and the ignition delay (Prakash and Ramesh [105]).
More detailed models for syngas/diesel dual-fuel combustion were based on the definition of ICE-compatible kinetics mechanisms, including diesel-syngas interaction [128] and ensuring reliable results in presence of turbulence, which is able to affect the ignition delay, flame stability and pollutant formation. To this end, Feng et al.[128] constructed a reduced mechanism accounting for syngas addition, and Stylianidis et al. [129] a new ICE-compatible syngas mechanism that was validated in terms of in-cylinder pressure profiles. The kinetic mechanisms were then introduced in the 3-D engine model, including other sub-models. In particular, the atomisation process was modelled by the Reitz-Diwakar model [130, 131] in Ref. [129], while Costa et al. [132] applied a droplet dynamics sub-model by O'Rourke [133], a coalescence model by Nordin [134] and the Dukowicz model [135] for droplets evaporation. Feng et al. [128] used the Kelvin-Helmholtz/Rayleigh-Taylor hybrid model [136]. Turbulence was simulated by means of two equations closure models [129]. The turbulence model must provide the turbulence-chemistry interaction. As an example, the ECFM model applied by Costa et al. [132] was used to account for the wrinkling of the flame front in turbulent regime.
Even with accurate simulation models, the setup of good operating parameters is a difficult task, as a complete parametric study requires a large number of numerical simulations. Rinaldini et al. [137] made this effort to draw a correlation for the best injection timing as a function of the diesel replacement rate. Chuahy et al. [112] tried to reduce the computational cost through a recursive use of Design of Experiments (DOE) and a Genetic Algorithm (GA). Both methods were applied to achieve successive refinements of the response surface. The CFD solver was used only after a good estimation of the optimum setup, with a considerable reduction of the computational time. A multi-objective optimization of

Corresponding Author: vinicio.magi@unibas.it

the engine parameters was also carried out in Ref. [111], to reduce the engine specific consumption and increase turbulence intensity at low and mean loads. The results of [111] are impressive for the large number of details provided by the procedure, although the authors do not provide any information on the computational cost.
These advanced numerical analysis clearly show that optimization algorithms are essential tools to obtain a more accurate picture of the engine performances. On the other hand, the number of simulations required to get optimal solutions may result too large for industrial contexts. In the near future, an efficient coupling of CFD, optimization and feedback control techniques will be an absolute requirement to achieve good results with reasonable computational costs.

2 Syngas as a fuel for HCSI engines

A large number of studies employed both numerical and experimental approaches to analyse the performance of homogeneous charge spark-ignited engines fuelled with syngas. Mixing of air and fuel takes place inside a carburettor or immediately before the intake valve for carburetted and port-injection SI engines, respectively. Indeed, this strategy typically assures the advantage of a good mixing of the charge. By contrast, this procedure generally limits the engine volumetric efficiency, since the gaseous fuel is characterized by a low density that limits the amount of air that can be introduced into the cylinder. Moreover, the fuel injected before the intake influences the indicated work due to pumping losses and emphasizes the heat losses through the cylinder walls.
The use of syngas as a fuel in carburetted and port-injection engines requires specific modifications of the tested engines to run with such a fuel. The experimental investigations generally provide pressure and heat released rate profiles, which are useful to analyse the combustion process as well as the ignition delay. Moreover, emissions of the main pollutants are also measured to quantify the advantage of syngas in terms of pollution abatement with respect to standard fuels. Thus, the engine performances are compared to those obtained with the use of traditional fossil fuels as either diesel or gasoline. The experiments are often aimed at identifying knock operating conditions to estimate the maximum compression ratio. However, results and conclusions reached by various authors may differ. The reason essentially depends on different characteristics of the tested engines and on the specific syngas composition, which can be strongly different from one to another, depending on the feedstock properties and on the gasifying agent.
The analyses reveal that this fuel could be efficiently used under lean conditions, which ensure low emissions of nitrogen oxides and low fuel specific consumptions. High compression ratios are often selected to improve the performance of this kind of engine. Despite these merits, the power output is still lower than that obtained with gasoline engines, and the trade-off between nitrogen oxides and carbon monoxide emissions and the low volumetric efficiency remain unresolved issues. Indeed, researchers are still trying to investigate new solutions.
In the following, scientific contributions dealing with the use of syngas in HCSI engines are discussed by considering several issues related to the engine performance and emissions.

2.1 Increase of compression ratio and knocking analysis

The use of a fuel having a low heating value leads to a sensible reduction of maximum in-cylinder pressure, especially under lean conditions, and a consequent reduction of IMEP. To overcome this issue, an attempt is to increase the compression ratio unless knock conditions are detected.
Several works in the available literature are devoted to identify the range of operating conditions that avoids knock triggering. This kind of analysis was carried out by Sridhar [138], who analysed the use of producer gas in spark-ignition engines. In his work, the compression ratio was changed from 17 to 11.5 to evaluate the engine performance for both low and high ratios[5]. The investigations revealed the absence of knock by using producer gas as fuel, even at high compression ratios. The engine always operated smoothly, without knock triggering, and this was ascribed to the fast H_2 burning rates and to the particular combustion chamber geometry. The author found higher efficiencies by operating at high compression ratios, although these benefits weaken beyond a certain value, at which friction losses start to predominate. This is the main reason to limit the compression ratio rather than knocking. The low knocking attitude of syngas combustion was also highlighted by Ahrenfeldt [139], who enhanced the

[5]The engine geometry was also modified to implement the spark plug and a hemispherical bowl was created on the piston head. This bowl showed a significant impact on the engine performance, especially on heat losses.

Corresponding Author: vinicio.magi@unibas.it

engine compression ratio to run with producer gas for power and heat production. Rakopulos and Michos [140] used a knock sub-model to evaluate the chance of knock triggering in all the examined test cases. A moderate risk of knocking was observed under full load operation at the maximum pressure peak. Their results showed a higher knocking dependence on the in-cylinder pressure than on the in-cylinder temperature.
Beside the compression ratio, the engine knocking attitude depends on the richness of the mixture, forcing to limit the equivalence ratio to avoid the engine damage. Marculescu et al. [141] increased the air-excess-ratio to 2.2-2.8 to avoid detonation in presence of syngas, due to the high H_2 reactivity. Bika et al. [142] analysed knock triggering as a function of syngas composition, equivalence ratio and compression ratio, using a CFR (Cooperative Fuel Research) engine fuelled with various mixtures of hydrogen and carbon monoxide. The analysis showed that the maximum allowed compression ratio to avoid knock risks decreases with the equivalence ratio (Figure 16), whereas the knock resistance increases with the CO fraction, as high CO percentages involve a less reactive behaviour of the entire mixture. It is then possible to take advantage of this knocking resistance by using very high compression ratios, which can improve the thermal efficiency of the engine. Anyway, carbon monoxide could also lead to low combustion efficiencies and the toxic and contaminant nature of CO compels to focus on the exhaust gas composition, beside the engine performances.

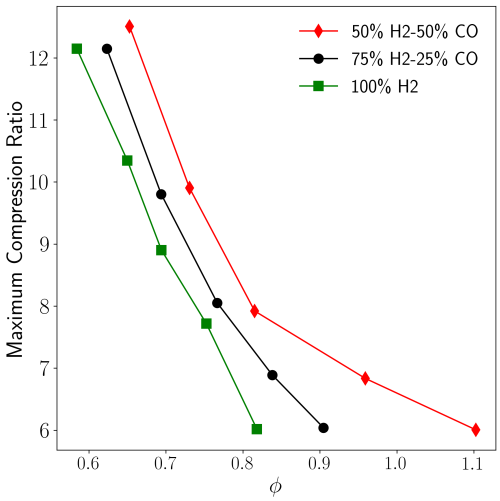

Figure 16: Maximum compression ratio as a function of the equivalence ratio and of the mixture composition [142].

2.2 Emissions in HCSI engines

The standards of the major European States in terms of emissions make difficult to spread the use of producer gas for power or heat generation in spark-ignition engines. This is mainly due to the difficulties in controlling NO_x and CO emissions at the same time.
The benefits in terms of emissions are generally discussed through a comparison with those produced by other fuels, such as methane, natural gas or gasoline. In some cases, NO_x decreases if syngas replaces gasoline. However, the increase of nitrogen oxides is usually observed when syngas replaces natural gas. On the other hand, CO emissions could be either higher or lower compared to those produced by conventional fossil fuels, as they strongly depend on the richness of the mixture and the oxygen distribution in the combustion chamber. Table 6 and 7 summarize the main results in terms of emissions obtained by several authors dealing with syngas.
Comparing the detected emissions with the existing regulations is utmost important to assess the feasibility of this technology. In particular, Sridhar et al. [143] carried out an extensive comparison with the emission standards in USA, Europe, Japan and India regarding CO, NO_x, HC and particulate matter (PM). They measured the emissions produced by three engines (E1, E2, E3) differing for the compression ratio set, the shape and the volume of the combustion chamber and the location of the spark plug. The engines E2 and E3 employed the adapted producer gas carburettor previously mentioned. Emission measurements showed NO_x emissions significantly lower than the current limits in case of producer gas.

Corresponding Author: vinicio.magi@unibas.it

Conversely, the emission of CO was above the standards with the engine E1, although the regulations are met by the engines E2 and E3 with the use of the adapted carburettor. This emphasizes the need of using specifically developed systems to handle syngas, and also suggests that the emissions and performance measured with gasoline engines fuelled by syngas could be unrepresentative of the effective benefits of this technology.
In the limiting conditions of no load[6], emissions of NO_x and CO were measured by Meng et al. [144], who found values under the standard Chinese limits for all the engine speeds under consideration.
Ahrenfeldt [139] compared the emissions detected in the Harboore, Gussing and Viking plants with the Denmark limits. In the Harboore and Viking plants both the emissions of NO_x and CO were below the standard. The high NO_x emissions detected in the Gussing plant were attributed to the high NH_3 content in the producer gas used to feed the engine. Based on the influence of the ignition advance on the NO_x generation, an ignition delay was therein proposed to control NO_x, although this strategy would increase the CO emissions due to incomplete combustion. This dependence on the ignition timing was not detected by Gobbato et al. [81], who changed the ignition timing from 29° to 23° BTDC. Hence, it is still not clear if the optimisation of the ignition timing could be an effective strategy to control NO_x emissions and meet the environmental standards. On the other hand, the NO_x and CO values recorded by Ahrenfeldt [139] with different ignition timings do not seem to form a well-established trend (Figure 17) due to the variability of the producer gas composition.

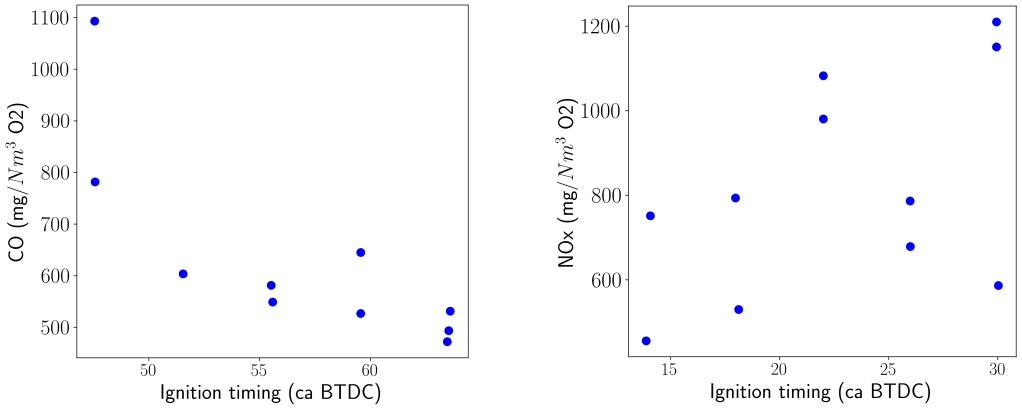

(a) CO (b) NO_x

Figure 17: Emissions measured by Ahrenfeldt [139] as a function of the ignition timing.

Beside the comparison with the environmental standards, the comparison of syngas emissions with those produced by common fossil fuels is a recurring topic in the available literature. Dai et al. [145] compared the emissions obtained with pure gasoline with those obtained with the addition of 2.5% of syngas. At the same air-to-fuel ratio under lean conditions, NO_x emissions are higher in case of syngas addition (Figure 18b), due to the wider range of flammability and its consequent higher cylinder temperatures for a given λ. As indicated in Figure 18a, CO emissions were also higher for syngas-blended gasoline engines, as the fast combustion of hydrogen consumes part of the necessary O_2 to oxidise the CO molecules. An interesting solution to prevent high NO_x emissions of hybrid syngas-gasoline engines was presented by Ji et al. [146], who produced syngas from ethanol catalytic decomposition. The decreasing NO_x emissions with the increase of the syngas volume fraction at fixed air-to-fuel ratio depend on the corresponding decrease of the oxygen concentration in the total intake. In addition, the produced syngas contained a significant fraction of ethanol, which contributed to reduce the maximum temperature achieved. As regards CO emissions, the authors found an increase of CO due to the generation of lean oxygen regions, the reduced overall combustion duration and the ethanol evaporation that subtracts energy to CO oxidation. Gasoline and syngas were also compared at the same ϕ in Ref. [147], whose results are shown in Figures 18 and 19. With respect to the above studies [145, 146], the measurements show a decrease of the NO_x emissions in case of syngas (see Figure 18b). These works show that for

[6]Analyses under no load conditions are particularly important to extend syngas engines to automotive applications, where these conditions are frequent.

small gasoline substitution rates (e.g. 2.5%), the increase of the laminar flame speed prevails, whereas for high or complete replacements (e.g. 100%) the reduced LHV leads to lower cylinder temperatures, hence also lower NO_x. On the other hand, CO emissions resulted slightly higher in Ref. [147] compared to gasoline for $0.7 < \phi < 0.8$.
However, when syngas and gasoline are compared at the same power output, the results are encouraging: Shah et al. [148] found 54-84% lower NO_x under syngas operation than under gasoline operation due to the lower temperature achieved during combustion. The reduction of 30-96% of CO was attributed to the lower carbon content in syngas compared to gasoline.
Other comparisons with gasoline, methane, biogas (Arroyo et al. [149]) and with gasoline and natural gas (Mustafi et al. [82]), at the same engine speed, showed that NO_x emissions are maximum for syngas, due to the H_2 content and the increased flame temperature. This increase of NO_x emissions due to the high H_2 reactivity could be partly balanced by the inert content in syngas, as in case of "syngas1" of Ref. [149]. In Ref. [149], "syngas 2" and gasoline also lead to the maximum CO emissions, which increased with the air-to-fuel ratio due to incomplete combustion. This trend was substantially different from those of methane and gasoline, whose CO emissions tend to decrease with λ. Conversely, Mustafi et al. [82] found the lowest CO emission under syngas operation, indicating a complete combustion. It is thus clear that the trends experienced for these emissions are difficult to generalise, as they are strictly related to the operating conditions applied and to the efficiency of the combustion process. Figure 18 summarizes the comparisons between syngas and gasoline emissions carried out by different authors for λ ranging from 1.0 to 1.4. The trade-off between NO_x and CO is clearly shown in the figure. Lean conditions are suggested to reduce NO_x, whereas CO emissions are considerably lower with gasoline at $\lambda = 1.0$.
A comparison with natural gas was carried out by Gobbato et al. [81], revealing lower emissions under syngas operation in terms of both CO and NO_x. The emissions of an engine fuelled with producer gas enriched with methane (0-60%) were detected by Szwaja et al. [150], who found comparable emissions of syngas and methane-blended syngas at the same equivalence ratio, as well as comparable peak pressures, temperatures and oxygen distributions. This similarity in terms of exhaust NO_x and CO can be also found in the results of Arroyo et al. [149], especially under lean conditions (ϕ=0.7-0.8) and with syngas containing a significant amount of inerts ("syngas 1", Table 8).
The above works usually identify the hydrogen content in syngas as the major factor explaining the emissions of NO_x. In particular, NO_x and CO pathways seem not to interact during combustion, following opposite trends only related by the oxygen availability in the combustion chamber: NO_x generation is enhanced by the H_2 reactivity, which, on the other hand, is able to subtract oxygen molecules for the CO oxidation. However, the study of Samiran et al. [151] on a premixed swirl flame combustor suggested a more complex interaction between such pollutants, whose synergy could be significant in some cases. The emissions of the combustor were examined for high (H_2/CO=3) and moderate (H_2/CO=1.2) H_2-rich syngas. Their results showed higher NO_x emissions with moderate H_2-rich syngas than those produced by the high H_2-rich fuel at the equivalence ratios tested (0.4-1.21). The influence of the CO content in the NO_x generation was then underlined: the CO molecules contribute to generate free oxygen via dissociation, and the C and H radicals needed to form the precursor HCN. Their results encourage the use of H_2 rich mixtures to control both CO and NO_x emissions at the same time, although it is not clear if this synergic behaviour could play a significant role also in engine combustion.
As seen in Table 6 and 7, syngas always leads to higher CO_2 emissions compared to traditional fossil fuels, mainly due to the relatively high CO_2 percentages in syngas and producer gas composition. As regards the HC emissions, they resulted generally negligible [149, 148] due to the very low amount of complex hydrocarbons in the fresh gas. However, in case of hybrid fossil fuels-syngas engines, syngas addition could lead to the incomplete burning of the mixture and the increase of the HC molecules coming from the traditional fuel.

Based on the above studies, a general statement is that benefits in terms of emissions are not always achieved for syngas engines. The main pollutant (NO_x and CO) production mechanisms are well understood, thus such emissions can be mitigated under different operating conditions with the use of appropriate combustion strategies.

Corresponding Author: vinicio.magi@unibas.it

Table 6: SI engines powered by syngas: emissions.

Operating conditions	**Ref.**	**NO_x**	**CO**	**CO_2**	**HC**
Three engines (E1, E2, E3), two of them employing a specifically developed carburettor (E2, E3)	Shridar et al. [143]	Increase with the ignition advance. Below environmental standards.	E1: above the environmental standards. E2, E3: the limits are met with the adapted syngas carburettor.	--	--
Harboore, Gussing and Viking plants (Denmark)	Ahrenfeldt [139]	Increasing with the ignition advance. The Harboøre and Viking plants meet the regulation in Denmark concerning both NOx and CO.	Increase with the ignition advance and the air to fuel ratio	--	Lower than the Denmark limits in all the cases
Comparison of gasoline, methane, biogas, syngas 1 and syngas 2 (Table 7)	Arroyo et al. [149]	Maximum with syngas2.	Maximum with syngas2 and gasoline at stoichiometric conditions.	High in case of syngas, partly due to its composition	Very low values detected with syngas
Comparison between syngas and gasoline	Shah et al. [148]	54-84% lower under syngas operation than under gasoline operation.	30-96% lower under syngas operation than under gasoline operation.	33-167% higher under syngas operation than under gasoline operation.	Negligible in case of syngas
Comparison between syngas and natural gas	Gobbato et al. [81]	Lower under syngas operation than under natural gas operation. No significant dependence on ignition advance	Lower under syngas operation than under natural gas operation. No significant dependence on ignition advance	--	--
Comparison between gasoline, natural gas and syngas	Mustafi et al. [82]	Highest under syngas operation.	Lowest under syngas operation (complete combustion)	Highest under syngas operation.	--

Corresponding Author: vinicio.magi@unibas.it

Table 7: SI engines powered by syngas: effects on emissions.

Operating conditions	**Ref.**	**NO_x**	**CO**	**CO_2**	**HC**
Two syngas enriched with hydrogen: moderate H2 -rich syngas (H2/CO=1.2) and high H2-rich syngas (H2/CO=3)	Samiran [151]	Higher in case of moderate H2-rich syngas than in case of high H2-rich syngas	Influence the NOx formation through dissociation and H, C radicals	--	--
Syngas addition (2.5%) to gasoline	Dai et al. [145]	Increase with syngas addition	Increase with syngas addition.	--	Lower with syngas addition at low airto-fuel ratios. Higher emissions with syngas addition for λ>1.2
Producer gas enriched with methane (0-60%)	Szwaja et al.[150]	Slightly affected by the methane content.	Slightly affected by the methane content.	Decrease with the methane content	Slightly affected by the methane content.
Hybrid gasolinesyngas engine. Syngas produced from ethanol catalytic decomposition	Ji et al. [146]	Decrease with the syngas volume fraction (ethanol)	Increase with the syngas volume fraction	--	Decrease with the syngas volume fraction.
Comparison between syngas (60% H_2, 40% CO), natural gas, ethanol and gasoline	Ran et al. [147]	For $0.7 < \phi < 0.8$ lower NO_x compared to gasoline, higher compared to natural gas and ethanol	Highly influenced by oxygen availability. Comparable emissions for all the fuels.	--	Negligible for syngas.
H_2-rich syngas compositions, no load conditions	Meng et al. [144]	Increase with the engine speed.	Increase with the engine speed.	--	Increase with the engine speed.

Corresponding Author: vinicio.magi@unibas.it

Table 8: Chemical composition and lower heating value (LHV) of the fuels employed by Arroyo et al.[149]

Fuel	**CO_2**	**CO**	**H_2**	**CH_4**	**LHV** [kJ/kg]
Methane	0	0	0	100	50200
Biogas	40	0	0	60	17717
Syngas 1	28	23	23	26	14095
Syngas 2	10	39	40	11	16525

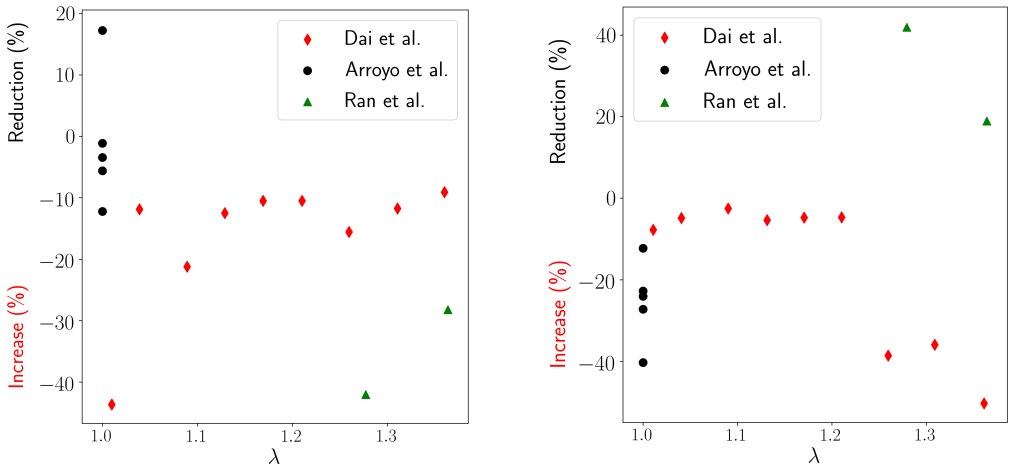

(a) CO (b) NO_x

Figure 18: Reduction of the emissions of CO and NO_x obtained with syngas, compared to gasoline fuelling. The results of Dai et al. [145] were obtained with a syngas replacement of 2.5%, while those of Arroyo et al. [149] and Ran et al. [147] in presence of pure syngas. The trade-off between NO_x ad CO emissions is clearly visible.

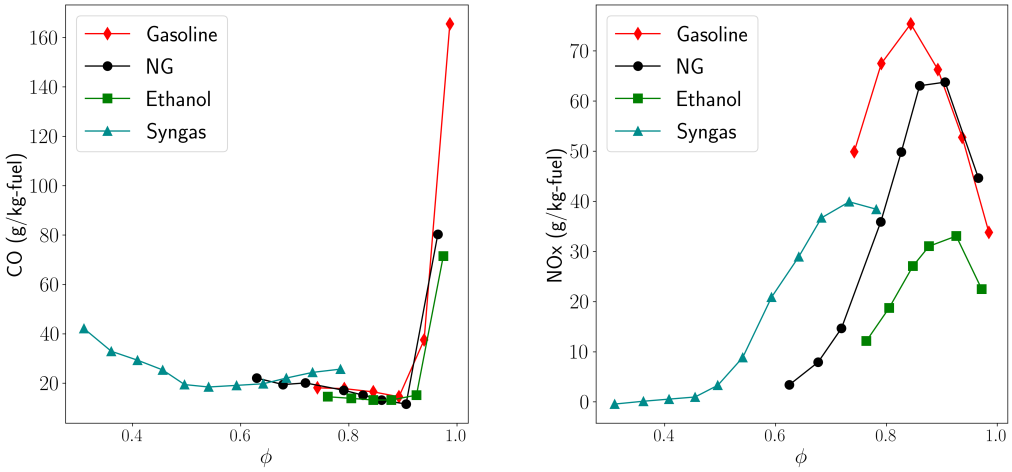

(a) CO (b) NO_x

Figure 19: Emissions of CO and NO_x detected by Ran et al. [147] in case of gasoline, ethanol, natural gas and syngas at several equivalence ratios.

2.3 Premixed flame propagation and engine performances

Syngas composition influences not only the engine emissions but also the premixed flame development and propagation, which in turn influences engine performances in terms of power output and efficiency. Hydrogen has the main role in flame propagation due to its high diffusivity, low molecular weight and high laminar flame speed. The hydrogen properties were also pointed out by Arroyo et al. [149] in their studies on gasoline, natural gas, syngas and biogas. They observed that syngas provided the fastest flame propagation, whereas biogas provided the slowest combustion process for all engine speeds. Ji et al. [146] found that both H_2 and CO fractions increase the production of radicals O and OH, which in turn increases the chain reactions rates of syngas combustion compared to gasoline combustion. Cribick et al. [152] replaced natural gas with syngas and found an increase of the brake torque, although *Syngas2* had a lower LHV compared to natural gas. Also in this case, the improvement of the performance was ascribed to the faster combustion and the reduced ignition delay related to the H_2 content.
This high H_2 reactivity often suggested a reduction of the ignition advance to increase the engine performance. This is an interesting question, as near stochiometric conditions the high hydrogen flame speed could have a negative impact on the efficiency since the pressure peak is moved too close to TDC. Mustafi et al. [82] adjusted the spark timing to obtain the maximum brake torque for each operating conditions with gasoline, natural gas and syngas. The optimal ignition timing for powergas was set near TDC due to the very fast syngas combustion. Also, Shridar and Yarasu [138] searched for the optimal ignition timing for syngas, which was delayed with respect to the natural gas ignition timing. Arroyo et al. [149] observed that the hydrogen contained in "syngas 1" and "syngas 2" (Tab. 8) gave higher pressure peaks, which moved towards TDC. Hence, the previous ignition timing, designed for gasoline fuel operations, was delayed to optimize the engine running with syngas. The ignition timing was also investigated by Homdoung et al. [153] for an engine powered by producer gas. In contrast to the above cases, this fuel required a larger ignition advance compared to powergas due to the low H_2 fraction and to the high inert content. The optimal ignition timing was found between 20° and 25° BTDC at 1100 rpm, and it had to be further advanced with the engine speed.

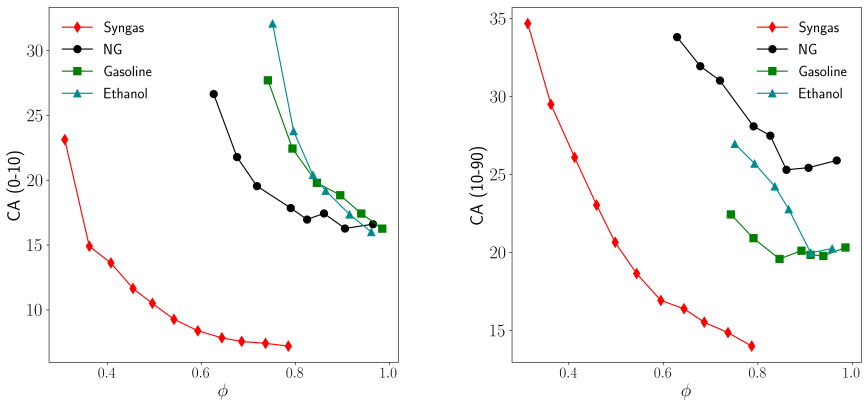

(a) Ignition delay (b) Rapid burn angle

Figure 20: Ignition delay time and rapid burn angle measured by Ran et al. [147] with ethanol, syngas, natural gas and gasoline with ϕ ranging from 0.4 to 1.0.

The combustion interval can be experimentally characterised with the use of specific parameters, such as as the crank angle intervals between spark ignition and 10% of the overall heat release (ignition lag), and between 10% and 90% of the total heat release (rapid burn angle). Ji et al. [146] measured these parameters and they found that syngas addition to gasoline (λ=1.2) reduced both the ignition lag and the rapid burn angle due to the increased flame speed. The same parameters were measured by Bika et al. [142] and Ran et al. [147], whose results are shown in Figure 20 for different fuels. The figure shows that syngas provides the fastest combustion among the fuels considered in their analysis. Bika [142] measured these parameters with different syngas compositions (H_2/CO=100/0,75/25,50/50), three equivalence ratios (ϕ =0.6,0.7,0.8) and three compression ratios (6,8,10). The rapid burn angle and the ignition lag were affected by all the experimental parameters under investigation. In particular, the H_2

Corresponding Author: vinicio.magi@unibas.it

content and the CO content reduced and increased, respectively, the rapid burn angle and the ignition lag. Higher equivalence ratios and compression ratios also shortened both intervals.
Syngas combustion appears also stable and characterised by low cycle to cycle variations (COV), as indicated by Arroyo et al. [149], whose results for different fuels are depicted in Figure 21. Indeed, this experimental campaign showed a stable combustion even at low loads and engine speeds, without any events of misfiring, which were typical of methane and biogas at the same equivalence ratios.

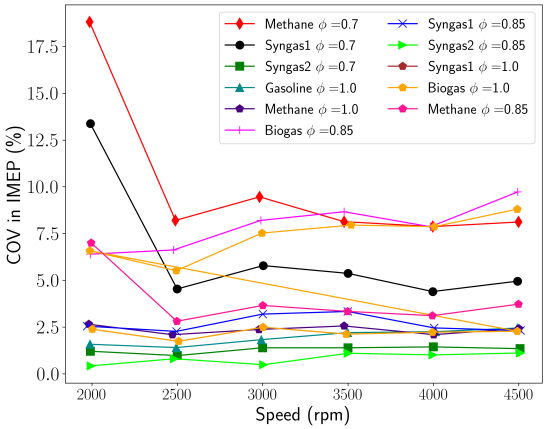

Figure 21: Coefficient of variation of IMEP by Arroyo et al. [149] with different fuels.

Such a stable combustion mode makes syngas particularly advantageous under lean conditions. Arroyo et al. [149] found the highest efficiencies with syngas at lean conditions, when the reduction of fuel consumptions prevailed on the worsening of the combustion process. Indeed, Mustafi et al. [82] chose a quasi-stoichiometric mixture for gasoline and natural gas operations, whereas lean conditions were selected for syngas. Dai et al. [145] measured an increase of the engine efficiency from 35.88% to 39.54% with syngas addition (2.5%) under lean conditions. Ahrenfeldt [139] also examined the performance of the syngas fuelled engine at various loads. The trends of the obtained power output and the engine efficiency with the richness of the mixture are recognisable, despite the variations of the producer gas composition. The increase of the air-to-fuel ratio led to a significant power decay, with a small decreases of the engine efficiency. The operating range of the engine was then extended under syngas operation, resulting into a maximum air-to-fuel ratio of 3.0 for producer gas, compared to the 1.8 of the natural gas. The best results in terms of burnt mass fraction were obtained with producer gas at specific air-to-fuel ratios of 1.4 and 1.6. A fairly constant thermal efficiency, with λ ranging from 1.2 to 2.5 (Figure 22), further supports the statement that producer gas is a good choice for lean burning combustion. Similar considerations were drawn by Ran et al., who decreased the equivalence ratio down to 0.3 with syngas. For $0.3 < \phi < 0.5$, the indicated thermal efficiency was the highest among those obtained with all the other fuels under consideration (i.e. gasoline, ethanol, natural gas) for near unity values of ϕ.
Even if improvements in terms of engine efficiency under lean conditions are observed, the engine power output and torque are generally lower compared to those obtained with conventional fossil fuels, due to the lower energy content of syngas. As an example, Sridhar and Yarasu [138] confermed a reduction of the engine power output of 16.7-26% for stochiometric and slightly rich mixtures, compared with that obtained under diesel operation. Indeed, the decrease of the energy content is only partially balanced by the increase of the premixed flame propagation. A decrease of the brake torque with the use of powergas was detected by Mustafi et al. [82], whose results are given in Figure 23. At lean conditions (ϕ=0.81) the decrease of torque was 23% and 30% for natural gas and gasoline, respectively, compared to nearly stoichiometric mixtures (ϕ=1.02-1.08). A decrease of the torque of 2% was observed by Chribik et al. [152], when a hydrogen volume fraction of 15% was added to natural gas (ϕ=1).
An increase of the specific fuel consumptions was also observed by Mustafi et al. [82], Papagiannakis et al. [154] and Chribik et al. [152], due to the very low stochiometric air-to-fuel ratio. As shown in Figure 23, Mustafi et al. [82] measured 3.4 times higher specific consumption with syngas than that with natural gas, while the consumption was 2.7 times higher with respect to gasoline. Chribik et al. [152] also found higher specific consumptions with syngas compared to hydrogen-blended natural gas. By increasing the inert content of syngas from 30% to 60%, an increase of the specific fuel consumptions

of 48% was also obtained.

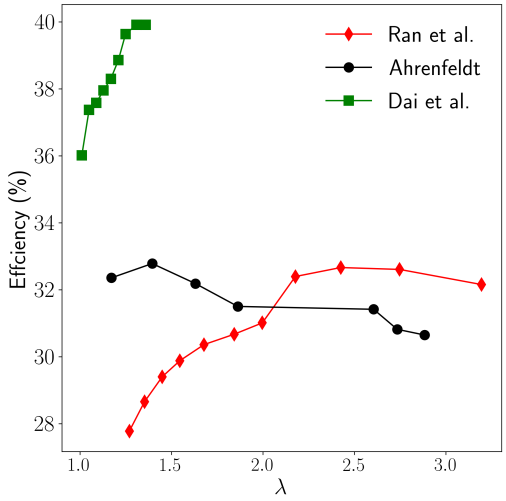

Figure 22: Efficiencies obtained by various authors with pure syngas [147, 139] and with a syngas addition to gasoline of 2.5 % (Dai et al. [145]).

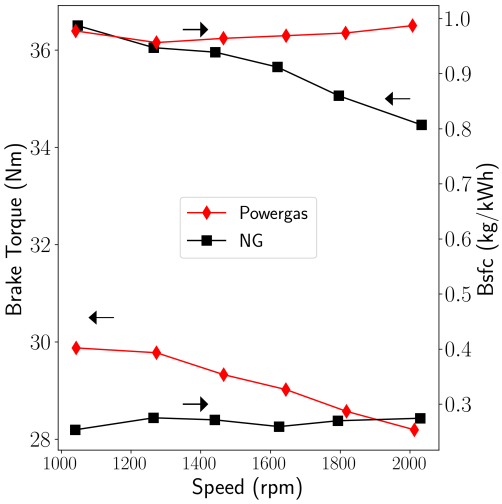

Figure 23: Brake torque and specific fuel consumption measured by Mustafi et al. [82] with syngas and natural gas.

2.4 Volumetric efficiency and heat losses

The heat transfer through the cylinder walls and the fluid dynamics of the intake process have also a strong impact on the engine performance. The intake is synthetically described by the volumetric efficiency of the engine, which depends on the light species content in the syngas, leading to a lower density of syngas compared to air density. In addition, syngas combustion is characterized by a very low stoichiometric air-to-fuel ratio (≃4.2) compared to natural gas (≃15.5) or gasoline (≃14.6). This means that a large amount of the cylinder volume is occupied by the fuel.
Figure 24a presents the results achieved by Mustafi et al. [82], who measured a reduction of the volumetric efficiency with syngas with respect to gasoline and natural gas. They also confirmed the influence of this parameter on the brake torque. The figure shows a relatively large difference of the volumetric efficiency by changing fuels. Gobbato et al. [81] noticed the same decrease in terms of volumetric efficiency and power de-rating by comparing syngas with natural gas. Ran et al. [147] stated that the low volumetric efficiency, together with the lower heating value, are responsible of the lowest IMEP obtained with syngas compared to gasoline, natural gas and ethanol. Figure 24b shows the volumetric efficiency with syngas which is always lower for any equivalence ratios.
As this effect is primarily related to the lower syngas density compared to air density, this difference clearly increases if syngas is at higher temperatures than ambient temperature. The temperature of the fresh gases was controlled by Ji et al. [146] by using ethanol as fixed stock for syngas production. The latent heat of vaporization of the residual ethanol contributed to reduce the intake temperature and to increase the volumetric efficiency of the engine. In such a way, the power output of the engine and its thermal efficiency increased.
Thermal efficiency also depends on heat losses. The improved thermal efficiency measured by Ji et al. [146] with syngas addition was ascribed to the faster combustion of syngas compared to gasoline, which reduced the post-combustion duration and the peak temperatures, as well as the heat transfer through the cylinder walls.
Conversely, Sridhar Yarasu [138] noticed higher heat losses with producer gas than those measured with diesel fuel, and Shivapuji and Dasappa [155] showed that the effect of the H_2 content in syngas was to enhance the engine cooling. While the first stage of combustion shortened due to the reduced energy requirements for ignition and the overall improvement of mixture reactivity, the second stage of combustion was longer due to enhanced cooling of the unburnt mixture along the boundary layers.
Direct injection could be an effective strategy to reduce the impact of these phenomena on engine performances. The volumetric efficiency would improve if syngas was injected after the inlet valve closing, as an increased amount of air would be introduced into the engine during the intake process.

Corresponding Author: vinicio.magi@unibas.it

Furthermore, a stratified charge could inhibit the formation of strong temperature gradients along the cylinder walls, thus reducing the heat losses.

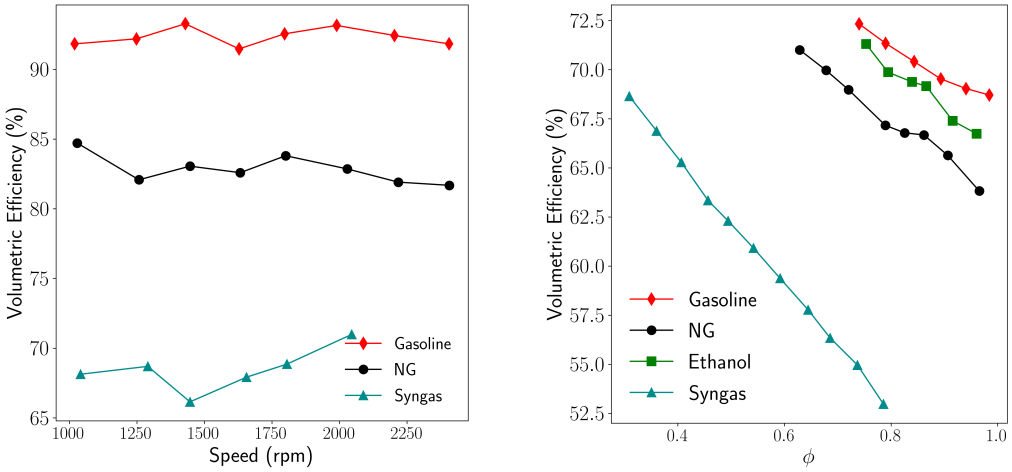

(a) Volumetric efficiency by Mustafi et al. [82]

(b) Volumetric efficiency by Ran et al. [147]

Figure 24: Volumetric efficiency by (a) Mustafi et al. [82] as a function of the engine speed, and by (b) Ran et al. [147] as a function of the equivalence ratio.

2.5 Numerical modelling of HCSI engines

Zero-dimensional models of HCSI engines fuelled by syngas were preferred in the past to multi-dimensional ones to obtain global integrated quantities. This approach was followed by Sridhar and Yarasu [138] as a first choice, and by Papagiannakis et al. [154]. The model described in Ref. [138] is based on the application of filling and emptying techniques for the intake and exhaust processes [106], the Eddy Entrainment and Laminar Burn-up model [156] for the heat-release process and the Annand's correlation [106] to model the heat losses. Turbulent parameters derived from 3-D cold flow simulations were employed to set the turbulent length scale and the turbulent intensity. This model is particularly simple, as it assumes an infinitely thin flame front, thus allowing to define two separate zones referring to unburnt and burnt gases. The model was applied to simulate a syngas fuelled engine characterised by a hemispherical bowl on the piston head with different compression ratios and equivalence ratios ranging from 1.0 to 1.25. The results showed a good agreement with experimental data with very early ignition timings. However, as the ignition was delayed, the agreement with the experimental results showed some discrepancies and the amount of the extra unburnt fuel considerably increased. The disagreement was attributed to the presence of an intense reverse squish during the expansion stroke, which is clearly not represented by the zero-dimensional model. The use of cold flow parameters to define turbulence variables is also questionable, as this model completely neglected the turbulence-chemistry interaction.
The partial ineffectiveness of a singular burning zone model was also assessed by Papagiannakis et al. [154], who carried out experiments on a multi-cylinder spark-ignited supercharged engine fuelled by syngas. They performed some measurements to validate a two-zone model, which was then employed to study the engine at various loads. The model is characterised by a wide use of empirical correlations to model the ignition process, laminar and turbulent flame speed, flame propagation and the heat transfer through the cylinder walls (Annand-type correlation [106]). Besides, chemical equilibrium reactions involving 11 chemical species and non-equilibrium models were considered to predict NO_x (Zeldovich mechanism [157]) and CO formation in the combustion chamber. The analysis also involved a knock sub-model based on an Arrhenius type equation to characterise knocking operating conditions. The validation procedure provided very low NO_x and CO emissions. Indeed, these pollutants could not be accurately estimated by a singular burning zone model: the lack of spatial and temporal resolution led the two-zone model to under estimate the actual temperature distribution with significant consequences on the NO_x predictions. The comparison against the experimental data in terms of CO also revealed the need of improving the sub-model for CO formation.
The above discrepancies led Rakopulos and Michos [140] to develop a multi-zone model based on the

definition of several different zones for the burning gas region, each of them representing the effect of temperature stratification, which has an important role in the NO_x formation. The model used a Wiebe's function to fit the experimental profile of the burnt fuel mass fraction. State equations and conservation equations for each single zone were applied to represent the burning gas region and the unburnt gas region. Heat transfer among the various zones was neglected by the model, whereas the global heat transferred to the cylinder walls was computed by using Annand's formula [106] . The validation of the multi-zone model was performed at full engine load. Then, the model was used to predict the amount of nitrogen oxygen at the exhaust valve opening (EVO). With this multi-zone model, the amount of NO_x can be computed for each zone as a function of the gas temperature history and the gaseous mass of the selected zone. This multi-zone approach provides an interesting improvement in the evaluation of NO_x compared to a singular burning zone, due to the more realistic description of the thermodynamic conditions occurring inside the combustion chamber. A sensitivity analysis was then performed to evaluate NO_x emissions by varying the number of burning zones, to ensure the independence of the results on this hyperparameter[7].

A multi-zone strategy was also adopted by Mustafi et al. [82] to perform a detailed emissions analysis. Their model is named ISIS (Integrated Spark Ignition engine Simulation) and is based on the routine developed by Ferguson [158]. The basic multi-zone model was extended to account for nitric oxide kinetics following the Zeldovich mechanism [157], while the other chemical concentrations were computed by assuming thermodynamic equilibrium. A good agreement between numerical and experimental results was obtained in terms of brake torque, with the computed torque slightly higher compared to the experimental one. This was attributed to the absence of other diluents beside nitrogen, which are expected to have a significant impact on the actual performance of the engine. A very good agreement was obtained in terms of O_2, CO_2 and CO emissions. NO_x were instead overestimated, although the model was able to follow the experimental trend over the entire range of air-to-fuel ratio.

Zero-dimensional models give the opportunity of studying complex systems by dividing them into a series of simplified zones. For example, Centeno et al. [159] developed a three zones model for the gasifier (drying and pyrolysis, oxidation and reduction zones) and used the multizone model proposed by Ferguson [158] for the engine. The model focused on the main performance parameters and did not involve any calculation of the pollutants. The coupled modelling of the gasifier and the engine enabled to study the whole "biomass-to-energy" conversion process, which is much more cumbersome to be investigatet with a detailed approach.

In another case [160], the system including a turbocharger, a charge cooling system and an engine was also numerically regulated by a PID controller. Kitanovic et al. [160] used the AVL BOOST IC simulation software to perform a parametric study involving fifteen simulations, with three different total engine displacements and five values of the excess-air-ratio. The heat transfer through the engine walls was modelled with the Woschini approach [127]. A Vibe-based heat release law was applied to model the combustion process: its closure constants were in turn modelled by a correlation developed by Carrera [161, 162] for biogas-fuelled engines. The presence of the controller allowed to vary the amount of fresh charge and the turbine size accordingly with the air-to-fuel ratio and the displacement imposed. The best operating parameters in terms of performance were then identified, although a knock sub-model was not included.

The limitations imposed by the zero dimensional modelling were partially overcome by Gamino and Aguillon [163], who built up a two-dimensional model capable to simulate the turbulent combustion of syngas in a diesel engine modified to gasoline operating conditions. This approach is based on solving the RANS equations on a very coarse, staggered grid (5 x 6 numerical cells) for 100 time steps, with a CPU time per combustion process lower than 1 s. The spatial discretisation identified 30 zones, although this multizone approach is substantially different from those presented before due to the integration of the partial differential governing equations. The combustion process was modelled by three global reactions, and a spark-ignition model was also implemented. The numerical model was validated by comparing the results with those obtained by Shridar [164] and Peters [165].

Fanelli et al.[166] obtained even more detailed results by simulating the CFR engine on a mesh of 570,000 grid points at TDC. The numerical model was based on the solution of the RANS equations: the standard k-ϵ model and a chemical kinetic mechanism [63] for syngas combustion were used to reproduce the experimental results of Bika et al. [142]. The model was developed in the Ansys Fluent environment and a partially premixed combustion model was employed, which included a flame propagation model (Extended Coherent Flamelet Model) together with a diffusion flame model (Steady Flamelet Model).

[7] It was shown that 5 zones should be enough to ensure reliable NO_x predictions, although this number would strictly depend on the effective temperature gradients achieved during combustion.

In addition, they provided new correlations for the laminar flame speed of various H_2 and CO mixtures with a good agreement with the experimental data. Such a model was then used by the authors to further investigate the CFR engine performance under various operating conditions.
The combustion model used by Fanelli et al. [166] was originally developed to deal with more complex cases, i.e. partially premixed combustion, where both premixed and diffusive burning regions can be identified in the combustion chamber. These circumstances were investigated by Zhang et al. [167], who carried out two-dimensional numerical simulations, involving detailed chemical kinetics and transport properties of a partially premixed engine, with a second injection of syngas before TDC. Their code was originally developed to deal with constant volume chambers, therefore source terms in the governing equations were introduced to include the effect of piston motion. The authors investigated the effect of the ratio between the fuel mass injected during the second stage and the premixed fuel mass.
More recently, three-dimensional CFD simulations of an engine fuelled with syngas were carried out by using STAR-CD v4.30 [168]. A single-cylinder, PFI, spark-ignited engine (AVL 5406) was considered, together with two pure syngas (H_2/CO) blends, i.e. 50/50 and 75/25 volume fraction of H_2/CO. An algebraic correlation for laminar flame speed was developed and validated for both syngas blends. The comparison with experiments showed that CFD simulations are able to predict the syngas combustion development with good accuracy, although the model needs for some improvements as regards the spark-ignition and the blow-by modelling.
3-D simulations of an SI engine fuelled with syngas and biogas were carried out by Kan et al. [169] by using KIVA-4 code. This model accounts for detailed chemistry by employing the GRI-Mech 3.0 mechanism, although no turbulence-chemistry interaction model has been considered. The results show a fluctuating heat release rate and a wider combustion interval compared to the experimental one.
The approaches presented in this section show that numerical models for syngas in HCSI engines have been considerably evolved in the past two decades. Nevertheless, current numerical techniques are still based on the solution of RANS equations, with a variety of submodels whose accuracy in engines should be carefully verified. In particular, high Reynolds number turbulence models, e.g. Standard k-ϵ model, simple gradient turbulence models for temperature, e.g. Reynolds Analogy, and species transport and flamelet approaches to treat the turbulence-chemistry interaction are very common choices. In principle, LES and DNS simulations could allow a more accurate description of the turbulent reacting flow structure within the engine combustion chamber, and would provide important findings to improve RANS models for these engines.

3 Syngas as a fuel for DI engines

In the last decades, direct injection of fuel is become one of the most common strategies for SI internal combustion engine. First of all, fuel direct injection does not place any restrictions to the amount of air that can be introduced in the cylinder, leading to significant improvements in terms of engine volumetric efficiency. Secondly, the direct injection of fuel is able to extend the operating range of the engine to leaner operating conditions.
An appropriate charge stratification is needed in this case to guarantee the ignition of the charge, which should be approximately stoichiometric where the spark takes place, to become leaner moving away from the spark plug. Lean operating conditions may also mitigate NO_x production due to the lower in-cylinder temperatures. In addition, the extended operating range allows a direct control of the output power by changing the amount of injected fuel. This limits the use of throttle to control the engine, so that pumping losses associated with the gas exchange process are reduced.
Despite the benefits that could be achieved, the literature still provides few works regarding syngas direct injection into SI engines. Very few works investigate syngas injection strategies, and chamber geometries to ensure an appropriate charge stratification are still far from being exhaustive. Hagos et al. [170, 171, 172] analyse the performance and the emissions of syngas fuelled direct injection engines and compare them with methane and natural gas engines.
In Ref.[170], the authors investigated the use of syngas for a direct injection engine and compared the results with those obtained by employing natural gas. The direct injection spark ignition (DISI) engine, developed by the Orbital company, had a compression ratio of 14:1 and a volume displacement of 399 cm^3. A syngas with 50% of hydrogen and 50% of carbon monoxide, in terms of volume fractions, was used for the experimental campaign. The indicated mean pressure was measured for several excess-air ratios, showing that the coefficient of variation of engine performances remained low since flame instabilities were damped by the low carbon monoxide flame speed. Syngas flammability range resulted wider than that of natural gas, whose coefficient of variation increased with the air-to-fuel ratio due to misfiring

Corresponding Author: vinicio.magi@unibas.it

events.
Lean conditions were considered due to the injection timing. Nevertheless, larger amounts of syngas should be injected into the combustion chamber to ensure similar engine performances with respect to natural gas, which has a higher heating value. The maximum injection time interval of 9 ms provided an air to fuel ratio of 1.5 under syngas fuelling mode. Hence, the engine cannot operate near stoichiometric conditions with, in addition, relatively low volumetric efficiencies. Indeed, most of the injection occurred during the intake valve opening. As a result, a significant amount of air left the cylinder during the injection process, as it was displaced by the injected low-density gas. This problem had important consequences on the overall efficiency of the engine.
The above difficulties led Hagos et al. [171] to analyse the influence of the starting of injection (SOI) timing on the engine performances. The start of injection was varied from 180° to 120° and 90° BTDC. As shown in Figure 25, the end of injection (EOI) was changed accordingly, depending on the engine speed.

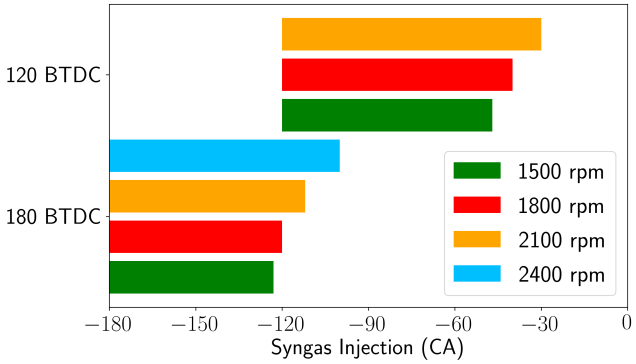

Figure 25: Injection durations set by Hagos et al.[171] for SOI of 180° BTDC and 120° BTDC at different engine speeds.

The same syngas composition given in Ref. [171] was used in Ref. [171], although it was enriched by a volume fraction of 20% of methane. Methane addition was necessary to increase the heating value of the fuel and consequently reduce the injection duration. As expected, the volumetric efficiency increased as the injection was delayed. Moreover, the engine performance also depended on the stratification achieved in the combustion chamber. At high engine speeds, the poor fuel-air mixing with SOI of 120° and 90° reduced the engine performances. Conversely, IMEP increased with the engine speed with SOI equal to 180°. On the other hand, higher heat released peaks occurred with retarded SOI due to the strong mixture stratification and the consequent lower heat losses. The SOI of 120° BTDC seemed to be the most economically favourable choice, although the advantages of this solution gradually vanished as the engine speed was increased. In particular, at high engine speeds the same performances in terms of efficiency were obtained with SOI equal to 120° and 180° BTDC.
Due to the significant volumetric losses, syngas enriched with methane (MES) was considered a good intermediate solution, and it was directly compared with pure syngas and natural gas in Ref. [172]. The advantages of pure syngas in terms of combustion efficiency were also found by using methane enriched syngas, which led to higher pressure and heat release peaks compared to CNG. Specifically, the maximum torque and thermal efficiency were reached with MES, as shown in Figures 26a and 26b. The increase of the engine thermal efficiency with the use of MES says that the thermal efficiency was more influenced by the combustion characteristics than by the lower heating value of the fuel. On the other hand, according with the content of low-density gas, the brake specific consumptions were maximum under syngas operating conditions and minimum under CNG operating conditions, with MES operating conditions in between (Figure 27).

The trade-off between NO_x and CO - HC emissions was also considered for the case of direct injection. Figure 28 shows that for syngas and MES, the emissions exceed those produced by natural gas at high (NO_x) and low (CO) loads. However, an intermediate load range (2.4 <BMEP< 3) can be identified, where the CO and NO_x emissions are comparable to those under natural gas operating conditions.
The injection timing significantly affect such emissions, as shown in Ref. [171] . Reduced injection timings led to higher CO and HC emissions due to incomplete combustion, with a further increase with the engine speed. SOI equal to 120° BTDC led also to large amounts of thermal NO_x associated with

Corresponding Author: vinicio.magi@unibas.it

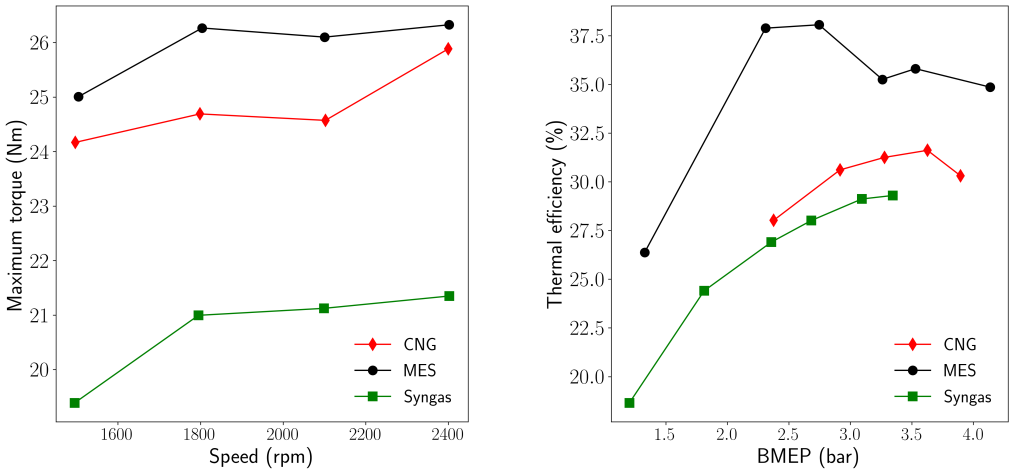

(a) (b)

Figure 26: Maximum brake torque (a) and thermal efficiency (b) measured by Hagos et al. [172] with natural gas, syngas and MES at 2100 rpm.

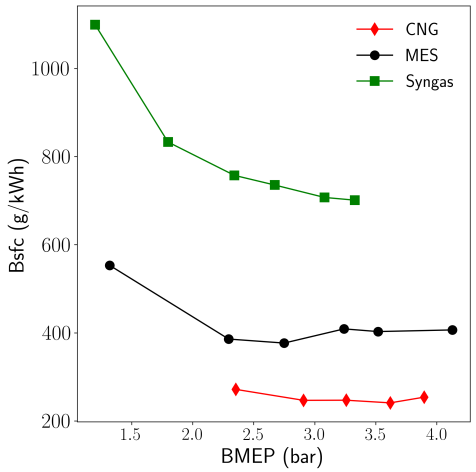

Figure 27: Brake fuel specific consumptions by Hagos et al. [172] for natural gas, syngas and MES at 2100 rpm.

the achieved high temperature . It is interesting to note that the best SOI in terms of performance was the worst from an environmental point of view.

Syngas direct injection potentially provides new design perspectives and innovative solutions concerning chamber geometries; specific injectors and operating parameters could possibly enhance the advantages and minimise emissions. The challenge is to confine the fuel within the burning region to avoid the formation of unburnt CO fuel under very lean operating conditions. Fiore et al. [173] numerically analysed the effect of piston shapes and injection specifications on the emissions and performance of a DISI engine fuelled by syngas. The parametric study involved three different piston cup geometries which are shown in Figure 29, and included half-angles of injection of 30°, 45°, 52.5° and 60°. The SOI timing was also varied from 90° BTDC to 130° BTDC. As shown in Figure 29, the piston shape considerably influenced the stratification: the Omega Combustion Cup (OCC) resulted the best choice in terms of performance, although it led to the maximum NO_x emissions. The trade-off between NO_x and CO emissions was not solved by this analysis, as unburnt CO emissions coming from incomplete combustion of syngas were significant in the cases with reduced thermal NO_x. The results were very sensitive to the injection angle and SOI, which influenced the fuel distribution. For some cases, the

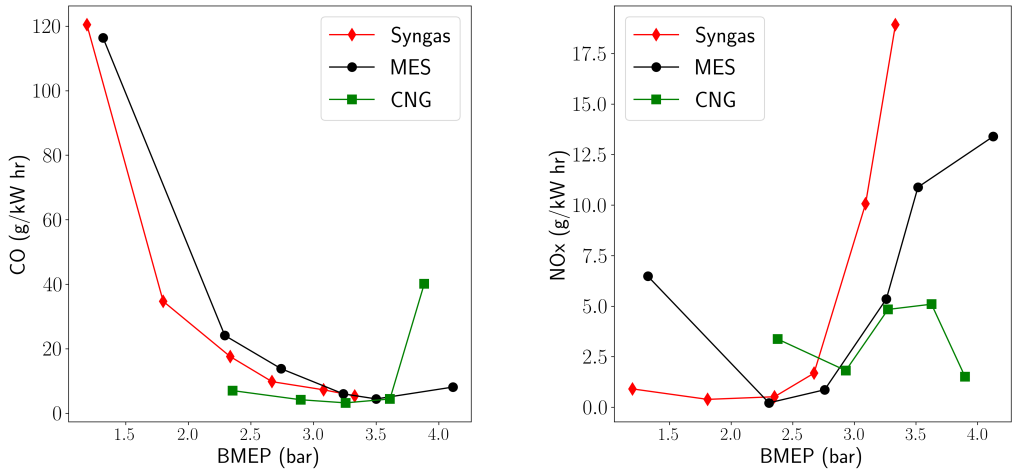

(a) CO (b) NO_x

Figure 28: Emissions of NO_x and CO by Hagos et al. [172] with natural gas, syngas and MES at 2100 rpm.

fuel distribution did not ensure an efficient flame propagation. Indeed, the equivalence ratio contours shown in Figure 29 suggested to place the spark plug in the main recirculation regions rather than on the cylinder axis.

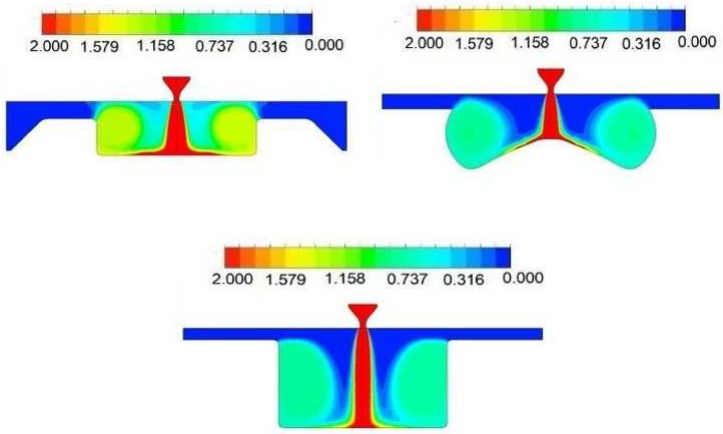

Figure 29: Equivalence ratio contour plots at 10° BTDC: (a) HCC; (b) OCC; (c) LCC [173].

However, this study was preliminary and a number of new configurations have to be explored to get strong conclusions. The high sensitivity on geometrical and operating parameters suggests to further search for optimal solutions.

Concluding Remarks

A critical review on the use of syngas for internal combustion engines over the last few decades has been provided. Internal combustion engines represent an extremely valid device for electricity, power and heat production. On the other hand, the emerging environmental issues require the use of new fuelling strategies for the engines. Syngas often represents the output of the disposal of wastes and plastic spoils, or it derives from wastes of the agrifood industry. In this context, syngas engines could be considered green and sustainable power units, whose supply is independent on oil multinational companies. The wide use of this hydrogen-based renewable fuel requires a complete renovation of the current energy network. Indeed, decentralization would be necessary towards rural areas or small communities offering

Corresponding Author: vinicio.magi@unibas.it

an appropriate supply of feedstocks to the power generation systems, without excessive transportation costs. It is likely that this revolution may have important social and economical implications.
So far, the use of syngas power generation systems is limited, in most of the cases, to small plants for recovery purposes. Indeed, modern industry is internalising the idea of environmental sustainability, and is looking forward to understanding the subsequent economic advantages. In this context, industry tends to appreciate internal energy recovery solutions. Industrial companies could use a gasification system for the disposal of industrial wastes and for the production of synthetic gas at the same time, thus reducing the external demand of energy carriers. The use of synthetic gas in engines could also significantly reduce greenhouse gases and hydrocarbons emissions. By means of an appropriate tuning of the operating engine parameters, carbon monoxide and nitrogen oxides emissions could be also mitigated if a specific gas composition is selected.
In view of these benefits, syngas combustion in internal combustion engines has been widely investigated in literature. Among the different types of engines, dual-fuel engines are very attractive due to their lower power derating with respect to syngas spark-ignition engines. The studies on dual-fuel engines show the possibility of achieving high diesel savings. High efficiencies with low emissions can be also obtained in the whole operating range with the use of appropriate strategies (Exhaust Gas Recirculation, reactivity control based on multiple injections, Premixed Combustion of the End-gas Region). Recently, efforts have been directed towards the optimization of these engines with advanced numerical techniques. However, the presence of two distinct fuel supply lines is a complexity that points up problems related to the storage and the transportation of the fuels. In addition, transient or failure scenarios, no load or abnormal conditions related to one of the fuel lines are not taken into account in the current works, although very likely to happen due to the limited predictability of syngas composition.
For Homogeneous Charge Spark-Igniton engines, the power derating is more consistent with respect to gasoline or natural gas. This decrease is a consequence of the low syngas heating value and the reduced volumetric efficiency, that can be only partially balanced by the increase of the compression ratio. Ultra-lean conditions become feasible in syngas operations, and contribute to reduce NO_x emissions. The improvement of these engines seems to lie in the use of turbocharged and supercharged SI engines, which so far are considered only in very few works. In particular, turbocharging will require new analysis as regards the engine knocking tendency and the maximum compression ratios and equivalence ratios to be used to avoid detonation.
Direct injection of syngas is a promising solution to avoid problems of poor filling, heat losses and incomplete combustion. Nevertheless, these studies are not yet conclusive as regard the definition of the optimal injection timing and ignition advances. In addition, very long injection durations represent a limit for the actual implementation of syngas direct injection. A way to overcome this problem is the use of specific syngas injectors (e.g. multi-holes injectors with large injection sections). Another way is the increase of the injection pressure. In this case, new experimental and numerical analysis need to be carried out to study the charge stratification. Economical analysis will be needed as well, to understand if the direct injection of syngas into the combustion chamber is effectively competitive with respect to other fuels.
For all types of engines, most of the analyses concern with a syngas composition with few species, even if this assumption may be not acceptable. Optimization methods with a large number of species will be more likely to provide accurate results.
Generally, the engine configurations in the literature are considerably different and the results are then rather difficult to compare. Hence, the definition of meaningful benchmarks appears as the best way to obtain a complete database, clarifying the effect of the operating parameters both qualitatively and quantitatively. Widely accepted benchmarks could also facilitate the validation of numerical models and to compare them in terms of efficiency and accuracy. This is rather important to formulate general simulation guidelines for syngas engines. Indeed, comprehensive parametric studies or submodels selection are not not always carried out. The development of simple correlations on the basis of experimental and numerical data would allow a faster design of recovery and power generation units.
Before treating numerical data as high fidelity data, Large-Eddy simulations or even Direct Numerical Simulations must be performed and numerical models need to be further improved and validated. In particular, models for turbulence-chemistry interaction should be tested to see their influence on the results obtained, especially in case of high speed direct injection of syngas. Multicomponent diffusion models based on Stefan-Maxwell or Ramshaw approximations should be included as well, since hydrogen diffuses much more faster compared to the other species contained in the mixture. Besides, the numerical models should account for the intake and exhaust processes, which are usually not under consideration in the simulations of syngas port-injection engines. Since a considerable fraction of the power derating is

Corresponding Author: vinicio.magi@unibas.it

related to the decrease of the volumetric efficiency, those processes should be included in the evaluation procedure. Uncertainty estimation for all the submodels involved in the simulations could be helpful to clarify the level of reliability of the results.
In the age of big data, machine learning techniques are expected to become increasingly important tools in all the scientific fields, including combustion in internal combustion engines with conventional or alternative fuels. Techniques of dimensionality reduction (e.g. Principal Component Analysis) could be applied to reduce the number of operating parameters to be changed, and to identify the patterns to be followed for a further optimization of syngas engines. Regression techniques as genetic programming or artificial neural networks could be helpful to construct specified submodels to handle syngas combustion. This is why the construction of wide and consistent databases is considered so important for future developments.
Besides, the integration of multiobjective feedback control strategies in CFD simulations would allow a reduction of the number of simulations required to properly optimize the operating parameters, also giving more realistic expectations as regard performance and emissions.
Nowadays, this technology seems to have reached a considerable level of technical development. The main skyline of the research on engines powered by syngas is then represented by the full optimization of these engines and the improvement of numerical models, whose standard use with respect to experimental approaches is rapidly increasing in both academic and industrial contexts.

Corresponding Author: vinicio.magi@unibas.it

References

[1] A. Malik and S.K. Mohapatra. Biomass-based gasifiers for internal combustion (ic) engines—a review. *Sadhana*, 38(3):461–476, 2013.

[2] N. Nipattummakul, I. Ahmed, S. Kerdsuwan, and A.K. Gupta. Hydrogen and syngas production from sewage sludge via steam gasification. *International Journal of Hydrogen Energy*, 35(21):11738–11745, 2010.

[3] F. Yan, S. Luo, Z. Hu, B. Xiao, and G. Cheng. Hydrogen-rich gas production by steam gasification of char from biomass fast pyrolysis in a fixed-bed reactor: Influence of temperature and steam on hydrogen yield and syngas composition. *Bioresource technology*, 101(14):5633–5637, 2010.

[4] M. He, B. Xiao, Z. Hu, S. Liu, X. Guo, and S. Luo. Syngas production from catalytic gasification of waste polyethylene: Influence of temperature on gas yield and composition. *International Journal of Hydrogen Energy*, 34(3):1342–1348, 2009.

[5] M. He, Z. Hu, B. Xiao, J. Li, X. Guo, S. Luo, et al. Hydrogen-rich gas from catalytic steam gasification of municipal solid waste (msw): Influence of catalyst and temperature on yield and product composition. *international journal of hydrogen energy*, 34(1):195–203, 2009.

[6] I.I. Ahmed, N. Nipattummakul, and A.K. Gupta. Characteristics of syngas from co-gasification of polyethylene and woodchips. *Applied energy*, 88(1):165–174, 2011.

[7] K. Li, R. Zhang, and J. Bi. Experimental study on syngas production by co-gasification of coal and biomass in a fluidized bed. *International journal of hydrogen energy*, 35(7):2722–2726, 2010.

[8] K. Sjöström, G. Chen, Q. Yu, C. Brage, and C. Rosén. Promoted reactivity of char in co-gasification of biomass and coal: synergies in the thermochemical process. *Fuel*, 78(10):1189–1194, 1999.

[9] A.G. Collot, Y. Zhuo, D.R. Dugwell, and R. Kandiyoti. Co-pyrolysis and co-gasification of coal and biomass in bench-scale fixed-bed and fluidised bed reactors. *Fuel*, 78(6):667–679, 1999.

[10] R.C. Brown, Q. Liu, and G. Norton. Catalytic effects observed during the co-gasification of coal and switchgrass. *Biomass and Bioenergy*, 18(6):499–506, 2000.

[11] Y.G. Pan, E. Velo, X. Roca, J.J. Manya, and L. Puigjaner. Fluidized-bed co-gasification of residual biomass/poor coal blends for fuel gas production. *Fuel*, 79(11):1317–1326, 2000.

[12] F. Pinto, C. Franco, R.N. Andre, C. Tavares, M. Dias, I. Gulyurtlu, and others. Effect of experimental conditions on co-gasification of coal, biomass and plastics wastes with air/steam mixtures in a fluidized bed system. *Fuel*, 82(15-17):1967–1976, 2003.

[13] E. Azzone, M. Morini, and M. Pinelli. Development of an equilibrium model for the simulation of thermochemical gasification and application to agricultural residues. *Renewable energy*, 46:248–254, 2012.

[14] C.R. Altafini, P.R. Wander, and R.M. Barreto. Prediction of the working parameters of a wood waste gasifier through an equilibrium model. *Energy Conversion and Management*, 44(17):2763–2777, 2003.

[15] H. Huang and S. Ramaswamy. Modeling biomass gasification using thermodynamic equilibrium approach. *Applied biochemistry and biotechnology*, 154(1-3):14–25, 2009.

[16] V.B. Silva and A. Rouboa. Using a two-stage equilibrium model to simulate oxygen air enriched gasification of pine biomass residues. *Fuel processing technology*, 109:111–117, 2013.

[17] S. Jarungthammachote and A. Dutta. Thermodynamic equilibrium model and second law analysis of a downdraft waste gasifier. *Energy*, 32(9):1660–1669, 2007.

[18] M. Simone, F. Barontini, C. Nicolella, and L. Tognotti. Assessment of syngas composition variability in a pilot-scale downdraft biomass gasifier by an extended equilibrium model. *Bioresource technology*, 140:43–52, 2013.

Corresponding Author: vinicio.magi@unibas.it

[19] H. Ghassemi and R. Shahsavan-Markadeh. Effects of various operational parameters on biomass gasification process; a modified equilibrium model. *Energy Conversion and Management*, 79:18–24, 2014.

[20] A. Mountouris, E. Voutsas, and D. Tassios. Solid waste plasma gasification: equilibrium model development and exergy analysis. *Energy Conversion and Management*, 47(13-14):1723–1737, 2006.

[21] N.S. Barman, S. Ghosh, and S. De. Gasification of biomass in a fixed bed downdraft gasifier–a realistic model including tar. *Bioresource technology*, 107:505–511, 2012.

[22] A. Silaen and T. Wang. Effect of turbulence and devolatilization models on coal gasification simulation in an entrained-flow gasifier. *International Journal of Heat and Mass Transfer*, 53(9-10):2074–2091, 2010.

[23] X. Ku, T. Li, and T. Løvås. Cfd–dem simulation of biomass gasification with steam in a fluidized bed reactor. *Chemical Engineering Science*, 122:270–283, 2015.

[24] N. Couto, V. Silva, E. Monteiro, S. Teixeira, R. Chacartegui, K. Bouziane, et al. Numerical and experimental analysis of municipal solid wastes gasification process. *Applied Thermal Engineering*, 78:185–195, 2015.

[25] C. Dong, B. Jin, and D. Li. Predicting the heating value of msw with a feed forward neural network. *Waste Management*, 23(2):103–106, 2003.

[26] G. Xiao, M. Ni, Y. Chi, B. Jin, R. Xiao, Z. Zhong, et al. Gasification characteristics of msw and an ann prediction model. *Waste Management*, 29(1):240–244, 2009.

[27] A. Pradhan, P. Baredar, and A. Kumar. Syngas as an alternative fuel used in internal combustion engines: A review. *Journal of Pure and Applied Science Technology*, 5(1):51–66, 2015.

[28] V.R. Kishore, M.R. Ravi, and A. Ray. Effect of hydrogen content and dilution on laminar burning velocity and stability characteristics of producer gas-air mixtures. *International Journal of Reacting Systems*, 310740, 2008.

[29] P. Ouimette and P. Seers. Numerical comparison of premixed laminar flame velocity of methane and wood syngas. *Fuel*, 88(3):528–533, 2009.

[30] C. Liu, B. Yan, G. Chen, and X. Bai. Structures and burning velocity of biomass derived gas flames. *International Journal of hydrogen energy*, 35(2):542–555, 2010.

[31] M. Fossum, R.V. Beyer, and IEA Bioenergy. Co-combustion: Biomass fuel gas and natural gas. *SINTEF Energy Research, Trondheim*, 1998.

[32] J. Natarajan and J.M. Seitzman. Laminar flame properties of h2/co mixtures. *Synthesis Gas Combustion: Fundamentals and Applications*, pages 71–98, 2010.

[33] E. Monteiro, M. Bellenoue, J. Sotton, N.A. Moreira, and S. Malheiro. Laminar burning velocities and markstein numbers of syngas–air mixtures. *Fuel*, 89(8):1985–1991, 2010.

[34] Y. Ai, Z. Zhou, Z. Chen, and W. Kong. Laminar flame speed and markstein length of syngas at normal and elevated pressures and temperatures. *Fuel*, 137:339–345, 2014.

[35] S. Ravi and E.L. Petersen. Laminar flame speed correlations for pure-hydrogen and high-hydrogen content syngas blends with various diluents. *International journal of hydrogen energy*, 37(24):19177–19189, 2012.

[36] J.M. Kuchta. Investigation of fire and explosion accidents in the chemical, mining, and fuel-related industries-a manual. bulletin. Technical report, Bureau of Mines, Washington, DC (USA), 1986.

[37] S. Li, Y. Zhang, X. Qiu, B. Li, and H. Zhang. Effects of inert dilution and preheating temperature on lean flammability limit of syngas. *Energy & fuels*, 28(5):3442–3452, 2014.

[38] H. Shih, J. Hsu, and Y. Lin. Computed flammability limits of opposed-jet h2/co syngas diffusion flames. *International journal of hydrogen energy*, 39(7):3459–3468, 2014.

Corresponding Author: vinicio.magi@unibas.it

[39] W.C. Gardiner, V.V. Lissianski, Z. Qin, G.P. Smith, D.M. Golden, M. Frenklach, et al. The grimechtm model for natural gas combustion and no formation and removal chemistry. In *5th Int. Conference on Combustion Technologies for a Clean Environment*, 1999.

[40] A. Kéromnès, W.K. Metcalfe, K.A. Heufer, N. Donohoe, A.K. Das, C. Sung, et al. An experimental and detailed chemical kinetic modeling study of hydrogen and syngas mixture oxidation at elevated pressures. *Combustion and Flame*, 160(6):995–1011, 2013.

[41] Z.M. Nikolaou, J. Chen, and N. Swaminathan. A 5-step reduced mechanism for combustion of co/h2/h2o/ch4/co2 mixtures with low hydrogen/methane and high h2o content. *Combustion and flame*, 160(1):56–75, 2013.

[42] R.K. Maurya, M.R. Saxena, A. Rathore, and R. Yadav. Chemical kinetic simulation of syngas-fueled hcci engine. In *Advances in Internal Combustion Engine Research*, pages 209–226. Springer, 2018.

[43] J. Herzler and C. Naumann. Shock tube study of the ignition of lean co/h2 fuel blends at intermediate temperatures and high pressure. *Combustion science and technology*, 180(10-11):2015–2028, 2008.

[44] A.M. Dean, D.C. Steiner, and E.E. Wang. A shock tube study of the h2/o2/co/ar and h2/n2o/co/ar systems: Measurement of the rate constant for h+ n2o= n2+ oh. *Combustion and Flame*, 32:73–83, 1978.

[45] J. Natarajan, T. Lieuwen, and J. Seitzman. Laminar flame speeds of h2/co mixtures: effect of co2 dilution, preheat temperature, and pressure. *Combustion and flame*, 151(1-2):104–119, 2007.

[46] A. Frassoldati, T. Faravelli, and E. Ranzi. The ignition, combustion and flame structure of carbon monoxide/hydrogen mixtures. note 1: Detailed kinetic modeling of syngas combustion also in presence of nitrogen compounds. *International Journal of Hydrogen Energy*, 32(15):3471–3485, 2007.

[47] R.A. Yetter, F.L. Dryer, and H. Rabitz. A comprehensive reaction mechanism for carbon monoxide/hydrogen/oxygen kinetics. *Combustion Science and Technology*, 79(1-3):97–128, 1991.

[48] T.J. Kim, R.A. Yetter, and F.L. Dryer. New results on moist co oxidation: high pressure, high temperature experiments and comprehensive kinetic modeling. In *Symposium (international) on combustion*, volume 25, pages 759–766. Elsevier, 1994.

[49] M.U. Alzueta, R. Bilbao, and P. Glarborg. Inhibition and sensitization of fuel oxidation by so2. *Combustion and Flame*, 127(4):2234–2251, 2001.

[50] A.K. Das, K. Kumar, and C. Sung. Laminar flame speeds of moist syngas mixtures. *Combustion and Flame*, 158(2):345–353, 2011.

[51] D. Singh, T. Nishiie, S. Tanvir, and L. Qiao. An experimental and kinetic study of syngas/air combustion at elevated temperatures and the effect of water addition. *Fuel*, 94:448–456, 2012.

[52] Y. He, Z. Wang, L. Yang, R. Whiddon, Z. Li, J. Zhou, et al. Investigation of laminar flame speeds of typical syngas using laser based bunsen method and kinetic simulation. *Fuel*, 95:206–213, 2012.

[53] S.G. Davis, A.V. Joshi, H. Wang, and F. Egolfopoulos. An optimized kinetic model of h2/co combustion. *Proceedings of the combustion Institute*, 30(1):1283–1292, 2005.

[54] S.D. Tse, D.L. Zhu, and C.K. Law. Morphology and burning rates of expanding spherical flames in h2/o2/inert mixtures up to 60 atmospheres. *Proceedings of the Combustion Institute*, 28(2):1793–1800, 2000.

[55] C.M. Vagelopoulos, F.N. Egolfopoulos, and C.K. Law. Further considerations on the determination of laminar flame speeds with the counterflow twin-flame technique. In *Symposium (international) on combustion*, volume 25, pages 1341–1347. Elsevier, 1994.

[56] O.C. Kwon and G.M. Faeth. Flame/stretch interactions of premixed hydrogen-fueled flames: measurements and predictions. *Combustion and Flame*, 124(4):590–610, 2001.

Corresponding Author: vinicio.magi@unibas.it

[57] E.L. Petersen, D.F. Davidson, and R.K. Hanson. Kinetics modeling of shock-induced ignition in low-dilution ch4/o2 mixtures at high pressures and intermediate temperatures. *Combustion and flame*, 117(1-2):272–290, 1999.

[58] E.L. Petersen. A shock tube and diagnostics for chemistry measurements at elevated pressures with application to methane ignition. 1999.

[59] P. Saxena and F.A. Williams. Testing a small detailed chemical-kinetic mechanism for the combustion of hydrogen and carbon monoxide. *Combustion and Flame*, 145(1-2):316–323, 2006.

[60] G. Balakrishnan, D. Trees, and F.A. Williams. An experimental investigation of strain-induced extinction of diluted hydrogen-air counterflow diffusion flames. *Combustion and Flame;(United States)*, 98, 1994.

[61] R. Seiser and K. Seshadri. The influence of water on extinction and ignition of hydrogen and methane flames. *Proceedings of the Combustion Institute*, 30(1):407–414, 2005.

[62] I.C. McLean, D.B. Smith, and S.C. Taylor. The use of carbon monoxide/hydrogen burning velocities to examine the rate of the co+ oh reaction. In *Symposium (international) on combustion*, volume 25, pages 749–757. Elsevier, 1994.

[63] H. Sun, S.I. Yang, G. Jomaas, and C.K. Law. High-pressure laminar flame speeds and kinetic modeling of carbon monoxide/hydrogen combustion. *Proceedings of the Combustion Institute*, 31(1):439–446, 2007.

[64] C.G. Fotache, Y. Tan, C.J. Sung, and C.K. Law. Ignition of co/h2/n2 versus heated air in counterflow: experimental and modeling results. *Combustion and flame*, 120(4):417–426, 2000.

[65] M.A. Mueller, R.A. Yetter, and F.L. Dryer. Kinetic modeling of the co/h2o/o2/no/so2 system: Implications for high-pressure fall-off in the so2+ o (+ m)= so3 (+ m) reaction. *International Journal of Chemical Kinetics*, 32(6):317–339, 2000.

[66] J. Li, Z. Zhao, A. Kazakov, M. Chaos, F.L. Dryer, and J.J. Scire Jr. A comprehensive kinetic mechanism for co, ch2o, and ch3oh combustion. *International Journal of Chemical Kinetics*, 39(3):109–136, 2007.

[67] W.C. Gardiner, M. McFarland, K. Morinaga, T. Takeyama, and B.F. Walker. Initiation rate for shock-heated hydrogen-oxygen-carbon monoxide-argon mixtures as determined by oh induction time measurements. *The Journal of Physical Chemistry*, 75(10):1504–1509, 1971.

[68] A.M. Starik, N.S. Titova, A.S. Sharipov, and V.E. Kozlov. Syngas oxidation mechanism. *Combustion, Explosion, and Shock Waves*, 46(5):491–506, 2010.

[69] J.V. Michael, J.W. Sutherland, L.B. Harding, and A.F. Wagner. Initiation in h2/o2: Rate constants for h2+ o2 yields h+ ho2 at high temperature. Technical report, ARGONNE NATIONAL LAB IL CHEMISTRY DIV, 2000.

[70] S. Ryu, S.M. Hwang, and M.J. Rabinowitz. Rate coefficient of the o+ h2= oh+ h reaction determined via shock tube-laser absorption spectroscopy. *Chemical physics letters*, 242(3):279–284, 1995.

[71] A.M. Starik, N.S. Titova, L.V. Bezgin, and V.I. Kopchenov. The promotion of ignition in a supersonic h2–air mixing layer by laser-induced excitation of o2 molecules: Numerical study. *Combustion and flame*, 156(8):1641–1652, 2009.

[72] A.M. Starik, B.I. Lukhovitskii, and N.S. Titova. Mechanism of the initiation of combustion in ch 4 (c 2 h 2)/air/o 3 mixtures by laser excitation of the o 3 molecules. *Kinetics and Catalysis*, 48(3):348–366, 2007.

[73] H.C. Hottel, G.C. Williams, N.M. Nerheim, and G.R. Schneider. Kinetic studies in stirred reactors: combustion of carbon monoxide and propane. In *Symposium (International) on Combustion*, volume 10, pages 111–121. Elsevier, 1965.

[74] F.L. Dryer and I. Glassman. High-temperature oxidation of co and ch4. In *Symposium (International) on combustion*, volume 14, pages 987–1003. Elsevier, 1973.

Corresponding Author: vinicio.magi@unibas.it

[75] J.A. Smith and G.J.J. Bartley. Stoichiometric operation of a gas engine utilizing synthesis gas and egr for no x control. *J. Eng. Gas Turbines Power*, 122(4):617–623, 2000.

[76] K. Vien. Experiments on the effect of exhaust gas recirculation diluent on the laminar burning speed and stability of syngas/air flames. 2016.

[77] S. Bhaduri, H. Jeanmart, and F. Contino. Tar tolerant hcci engine fuelled with biomass syngas: combustion control through egr. *Energy Procedia*, 105:1764–1770, 2017.

[78] T. Han, G. Lavoie, M. Wooldridge, and A. Boehman. Effect of syngas (h/co) on si engine knock under boosted egr and lean conditions. *SAE International Journal of Engines*, 10(3):959–969, 2017.

[79] D.K. Marsh and A.K. Voice. Quantification of knock benefits from reformate and cooled exhaust gas recirculation using a livengood–wu approach with detailed chemical kinetics. *International Journal of Engine Research*, 18(7):717–731, 2017.

[80] S. Bhaduri, H. Jeanmart, and F. Contino. Egr control on operation of a tar tolerant hcci engine with simulated syngas from biomass. *Applied Energy*, 227:159–167, 2018.

[81] P. Gobbato, M. Masi, and M. Benetti. Performance analysis of a producer gas-fuelled heavy-duty si engine at full-load operation. *Energy Procedia*, 82:149–155, 2015.

[82] N.N. Mustafi, Y.C. Miraglia, R.R. Raine, P.K. Bansal, and S.T. Elder. Spark-ignition engine performance with 'powergas' fuel (mixture of co/h2): A comparison with gasoline and natural gas. *Fuel*, 85(12-13):1605–1612, 2006.

[83] J. Fuchs, A. Leitner, G. Tinschmann, and C. Trapp. Concept for high-performance direct ignition gas engines. *MTZ worldwide*, 74(5):18–23, 2013.

[84] S. Dasappa and H.V. Sridhar. Performance of a diesel engine in a dual fuel mode using producer gas for electricity power generation. *International Journal of Sustainable Energy*, 32(3):153–168, 2013.

[85] T.R. Anil, S.D. Ravi, M. Shashikanth, N.K.S. Rajan P.G. Tewari, and N.K.S. Rajan. Cfd analysis of a mixture flow in a producer gas carburetor. In *International Conference On Computational Fluid Dynamics, Acoustics, Heat Transfer and Electromagnetics CFEMATCON-06*, 2006.

[86] K.S. Umesh, V.K. Pravin, K. Rajagopal, and P.H. Veena. Numerical validation of producer gas carburetor. 2012.

[87] R. Reddy and P. Reddy. Analysis of producer gas carburetor for different air-fuel ratios using cfd. *International Journal of Research in Engineering and Technology*, 3:470–474, 2014.

[88] S.L. Konde and R.B. Yarasu. Cfd simulation and geometrical optimization of producer gas carburetor. *IJETT*, 13(2):59–62, 2014.

[89] A. Kumar and A.K. Sharma. Design and development of gas carburettor for a gasifier-engine system. *Journal of The Institution of Engineers (India): Series C*, 98(2):83–89, 2017.

[90] N.R. Banapurmath, V.S. Yaliwal, S. Kambalimath, A.M. Hunashyal, and P.G. Tewari. Effect of wood type and carburetor on the performance of producer gas-biodiesel operated dual fuel engines. *Waste and Biomass Valorization*, 2(4):403, 2011.

[91] L.C.O Villalba and E.R. Acevedo. Technical and economical assessment of power generation technologies firing syngas obtained from biosolid gasification. *Producción+ Limpia*, 9(1):31–43, 2014.

[92] C.R. Coronado, J.T. Yoshioka, and J.L. Silveira. Electricity, hot water and cold water production from biomass. energetic and economical analysis of the compact system of cogeneration run with woodgas from a small downdraft gasifier. *Renewable Energy*, 36(6):1861–1868, 2011.

[93] R.A.M. Boloy, J.L. Silveira, C.E. Tuna, C.R. Coronado, and J.S. Antunes. Ecological impacts from syngas burning in internal combustion engine: Technical and economic aspects. *Renewable and Sustainable Energy Reviews*, 15(9):5194–5201, 2011.

Corresponding Author: vinicio.magi@unibas.it

[94] A.A. Dennetiere, F. Leorat, and G.F. Bonnici. Power generation from biomass residues using the gasifier/dual-fuel engine technique. ACS Publications, 1980.

[95] F. Vyarawalla, P.P. Parikh, H.C. Dak, and B.C. Jain. Utilisation of biomass for motive power generation—gasifier engine system. *Biomass*, 5(3):227–242, 1984.

[96] P.P. Parikh, A.G. Bhave, and D.V. Kapse. Study of thermal and emission performance of small gasifier-dual-fuel engine systems. *Biomass*, 19(1-2):75–97, 1989.

[97] P. Sombatwong, P. Thaiyasuit, and K. Pianthong. Effect of pilot fuel quantity on the performance and emission of a dual producer gas–diesel engine. *Energy procedia*, 34:218–227, 2013.

[98] B.K.M. Mahgoub, S.A. Sulaiman, and Z.A. Abdul Karim. Performance study of imitated syngas in a dual-fuel compression ignition diesel engine. *International Journal of Automotive & Mechanical Engineering*, 11, 2015.

[99] R. Uma, T.C. Kandpal, and V.V.N. Kishore. Emission characteristics of an electricity generation system in diesel alone and dual fuel modes. *Biomass and bioenergy*, 27(2):195–203, 2004.

[100] O. Nwafor. Knock characteristics of dual-fuel combustion in diesel engines using natural gas as primary fuel. *Sadhana*, 27(3):375–382, 2002.

[101] F. Khaled, J. Badra, and A. Farooq. Ignition delay time correlation of fuel blends based on livengood-wu description. *Fuel*, 209:776–786, 2017.

[102] H.O. Hardenberg and F.W. Hase. An empirical formula for computing the pressure rise delay of a fuel from its cetane number and from the relevant parameters of direct-injection diesel engines. *SAE Transactions*, pages 1823–1834, 1979.

[103] S. Ikura, T. Kadota, and H. Hiroyasu. Ignition delay of fuel sprays in a constant volume bomb. *Trans. JSME*, 41(345):1559–1568, 1975.

[104] C. Mansour, A. Bounif, A. Aris, and F. Gaillard. Gas–diesel (dual-fuel) modeling in diesel engine environment. *International Journal of Thermal Sciences*, 40(4):409–424, 2001.

[105] G. Prakash, A. Ramesh, and A.B. Shaik. An approach for estimation of ignition delay in a dual fuel engine. *SAE transactions*, pages 399–405, 1999.

[106] B. John. Heywood, internal combustion engine fundamentals. *Pub: McGraw Hill International Editions*, 1988.

[107] U. Azimov, E. Tomita, N. Kawahara, and Y. Harada. Effect of syngas composition on combustion and exhaust emission characteristics in a pilot-ignited dual-fuel engine operated in premier combustion mode. *international journal of hydrogen energy*, 36(18):11985–11996, 2011.

[108] C. Aksu, N. Kawahara, K. Tsuboi, M. Kondo, and E. Tomita. Extension of premier combustion operation range using split micro pilot fuel injection in a dual fuel natural gas compression ignition engine: A performance-based and visual investigation. *Fuel*, 185:243–253, 2016.

[109] A. Talekar, M. Lai, E. Tomita, N. Kawahara, K. Zeng, and B. Yang. Numerical investigation of natural gas-diesel dual fuel engine with end gas ignition. Technical report, SAE Technical Paper, 2018.

[110] M.M. Roy, E. Tomita, N. Kawahara, Y. Harada, and A. Sakane. Performance and emission comparison of a supercharged dual-fuel engine fueled by producer gases with varying hydrogen content. *International Journal of Hydrogen Energy*, 34(18):7811–7822, 2009.

[111] Z. Xu, M. Jia, Y. Li, Y. Chang, G. Xu, L. Xu, et al. Computational optimization of fuel supply, syngas composition, and intake conditions for a syngas/diesel rcci engine. *Fuel*, 234:120–134, 2018.

[112] F.D.F. Chuahy and S.L. Kokjohn. High efficiency dual-fuel combustion through thermochemical recovery and diesel reforming. *Applied energy*, 195:503–522, 2017.

[113] W.N.W. Mansor. *Dual fuel engine combustion and emissions-an experimental investigation coupled with computer simulation*. PhD thesis, Colorado State University, 2014.

Corresponding Author: vinicio.magi@unibas.it

[114] B.B. Sahoo, N. Sahoo, and U.K. Saha. Effect of h2: Co ratio in syngas on the performance of a dual fuel diesel engine operation. *Applied Thermal Engineering*, 49:139–146, 2012.

[115] H. Guo, W.S. Neill, and B. Liko. The combustion and emissions performance of a syngas-diesel dual fuel compression ignition engine. In *ASME 2016 Internal Combustion Engine Division Fall Technical Conference*. American Society of Mechanical Engineers Digital Collection, 2016.

[116] H. Singh and S.K. Mohapatra. Production of producer gas from sugarcane bagasse and carpentry waste and its sustainable use in a dual fuel ci engine: A performance, emission, and noise investigation. *Journal of the Energy Institute*, 91(1):43–54, 2018.

[117] S. Hassan, Z.A. Zainal, and M.A. Miskam. Effects of advanced injection timing on performance and emission of a supercharged dual-fuel diesel engine fueled by producer gas fromdowndraft gasifier. 2011.

[118] A.L. Boehman and O.L. Corre. Combustion of syngas in internal combustion engines. *Combustion science and technology*, 180(6):1193–1206, 2008.

[119] V. Shrivastava, A.K. Jha, A.K. Wamankar, and S. Murugan. Performance and emission studies of a ci engine coupled with gasifier running in dual fuel mode. *Procedia Engineering*, 51:600–608, 2013.

[120] A.S. Ramadhas, S. Jayaraj, and C. Muraleedharan. Power generation using coir-pith and wood derived producer gas in diesel engines. *Fuel Processing Technology*, 87(10):849–853, 2006.

[121] R.N. Singh, S.P. Singh, and B.S. Pathak. Investigations on operation of ci engine using producer gas and rice bran oil in mixed fuel mode. *Renewable Energy*, 32(9):1565–1580, 2007.

[122] C. Nayak, B.P. Pattanaik, and S.K. Nayak. Effect of preheated jatropha oil and jatropha oil methyl ester with producer gas on diesel engine performance. *International Journal of Automotive & Mechanical Engineering*, 9, 2014.

[123] N. Kashipura, N.R. Banapurmath, G. Manavendra, A.M. Nagaraj, V.S. Yaliwal, V. Kulkarni, et al. Effect of combustion chamber shapes on the performance of duel fuel engine operated on rice bran oil methyl ester and producer gas. *Journal of Petroleum & Environmental Biotechnology*, 6(225):1–8, 2015.

[124] V.S. Yaliwal, N.R. Banapurmath, N.M. Gireesh, R.S. Hosmath, T. Donateo, and P.G. Tewari. Effect of nozzle and combustion chamber geometry on the performance of a diesel engine operated on dual fuel mode using renewable fuels. *Renewable Energy*, 93:483–501, 2016.

[125] A.A.M. Ali, K. Ali, C. Kim, Y. Lee, S. Oh, and K. Kim. Numerical study of the combustion characteristics in a syngas-diesel dual-fuel engine under lean condition. *International Journal of Automotive Technology*, 20(5):933–942, 2019.

[126] C. Caligiuri and M. Renzi. Combustion modelling of a dual fuel diesel–producer gas compression ignition engine. *Energy Procedia*, 142:1395–1400, 2017.

[127] G. Woschni. A universally applicable equation for the instantaneous heat transfer coefficient in the internal combustion engine. Technical report, SAE Technical paper, 1967.

[128] S. Feng. Numerical study of the performance and emission of a diesel-syngas dual fuel engine. *Mathematical Problems in Engineering*, 2017, 2017.

[129] N. Stylianidis, U. Azimov, A. Maheri, E. Tomita, and N. Kawahara. Chemical kinetics and cfd analysis of supercharged micro-pilot ignited dual-fuel engine combustion of syngas. *Fuel*, 203:591–606, 2017.

[130] R.D. Reitz and R. Diwakar. Effect of drop breakup on fuel sprays. *SAE transactions*, pages 218–227, 1986.

[131] R.D. Reitz and R. Diwakar. Structure of high-pressure fuel sprays. *SAE transactions*, pages 492–509, 1987.

Corresponding Author: vinicio.magi@unibas.it

[132] M. Costa, M. La Villetta, N. Massarotti, D. Piazzullo, and V. Rocco. Numerical analysis of a compression ignition engine powered in the dual-fuel mode with syngas and biodiesel. *Energy*, 137:969–979, 2017.

[133] P.J. o'Rourke. Modelling of drop interactions in thick sprays and a comparison with experiments. *I. Mech. E., C*, 404(80):101–116, 1980.

[134] P. Nordin. *Complex Chemistry Modelling of Diesel Sprays*. PhD thesis, Ph. D. thesis, Chalmers University of Technology, Göteborg, 1995.

[135] J.K. Dukowicz. Quasi-steady droplet phase change in the presence of convection. Technical report, Los Alamos Scientific Lab., NM (USA), 1979.

[136] J.C. Beale and R.D. Reitz. Modeling spray atomization with the kelvin-helmholtz/rayleigh-taylor hybrid model. *Atomization and sprays*, 9(6), 1999.

[137] C.A. Rinaldini, G. Allesina, S. Pedrazzi, E. Mattarelli, and P. Tartarini. Modeling and optimization of industrial internal combustion engines running on diesel/syngas blends. *Energy conversion and management*, 182:89–94, 2019.

[138] G. Sridhar and R.B. Yarasu. Facts about producer gas engine. In *Paths to Sustainable Energy*. IntechOpen, 2010.

[139] J. Ahrenfeldt. Characterization of biomass producer gas as fuel for stationary gas engines in combined heat and power production. *MED, DTU. Kgs. Lyngby: sn*, page 127, 2007.

[140] C.D. Rakopoulos, C.N. Michos, and E.G. Giakoumis. Availability analysis of a syngas fueled spark ignition engine using a multi-zone combustion model. *Energy*, 33(9):1378–1398, 2008.

[141] C. Marculescu, V. Cenuşă, and F. Alexe. Analysis of biomass and waste gasification lean syngases combustion for power generation using spark ignition engines. *Waste management*, 47:133–140, 2016.

[142] A.S. Bika, L. Franklin, and D.B. Kittelson. Engine knock and combustion characteristics of a spark ignition engine operating with varying hydrogen and carbon monoxide proportions. *International journal of hydrogen energy*, 36(8):5143–5152, 2011.

[143] G. Sridhar, H.V. Sridhar, S. Dasappa, P.J. Paul, N.K.S. Rajan, and H.S. Mukunda. Development of producer gas engines. *Proceedings of the Institution of Mechanical Engineers, Part D: Journal of Automobile Engineering*, 219(3):423–438, 2005.

[144] F. Meng, H. Wang, Q. Ma, D. Wang, and J. Lin. Emission characteristics of vehicles fueled by hydrogen-enriched syngas under no-load condition. *International Journal of Hydrogen Energy*, 45(6):3840–3845, 2020.

[145] X. Dai, C. Ji, S. Wang, C. Liang, X. Liu, and B. Ju. Effect of syngas addition on performance of a spark-ignited gasoline engine at lean conditions. *International journal of hydrogen energy*, 37(19):14624–14631, 2012.

[146] C. Ji, X. Dai, S. Wang, C. Liang, B. Ju, and X. Liu. Experimental study on combustion and emissions performance of a hybrid syngas–gasoline engine. *International journal of hydrogen energy*, 38(25):11169–11173, 2013.

[147] Z. Ran, D. Hariharan, B. Lawler, and S. Mamalis. Experimental study of lean spark ignition combustion using gasoline, ethanol, natural gas, and syngas. *Fuel*, 235:530–537, 2019.

[148] A. Shah, R. Srinivasan, S.D.F. To, and E.P. Columbus. Performance and emissions of a spark-ignited engine driven generator on biomass based syngas. *Bioresource technology*, 101(12):4656–4661, 2010.

[149] J. Arroyo, F. Moreno, M. Muñoz, C. Monné, and N. Bernal. Combustion behavior of a spark ignition engine fueled with synthetic gases derived from biogas. *Fuel*, 117:50–58, 2014.

[150] S. Szwaja, V.B. Kovacs, A. Bereczky, and A. Penninger. Sewage sludge producer gas enriched with methane as a fuel to a spark ignited engine. *Fuel processing technology*, 110:160–166, 2013.

Corresponding Author: vinicio.magi@unibas.it

[151] N.A. Samiran, J. Ng, M.N.M. Jaafar, A. Valera-Medina, and C.T. Chong. H2-rich syngas strategy to reduce nox and co emissions and improve stability limits under premixed swirl combustion mode. *International Journal of Hydrogen Energy*, 41(42):19243–19255, 2016.

[152] A. Chríbik, M. Polóni, and J. Lach. Effect of gas mixture composition on the parameters of an internal combustion engine. 2012.

[153] N. Homdoung, N. Tippayawong, and N. Dussadee. Effect of ignition timing advance on performance of a small producer gas engine. *International Journal of Applied Engineering Research*, 9(13):2341–2348, 2014.

[154] R.G. Papagiannakis, C.D. Rakopoulos, D.T. Hountalas, and E.G. Giakoumis. Study of the performance and exhaust emissions of a spark-ignited engine operating on syngas fuel. *International Journal of Alternative Propulsion*, 1(2/3):190–215, 2007.

[155] A.M. Shivapuji and S. Dasappa. Influence of fuel hydrogen fraction on syngas fueled si engine: Fuel thermo-physical property analysis and in-cylinder experimental investigations. *international journal of hydrogen energy*, 40(32):10308–10328, 2015.

[156] J.C. Keck. Turbulent flame structure and speed in spark-ignition engines. In *Symposium (International) on Combustion*, volume 19, pages 1451–1466. Elsevier, 1982.

[157] C. Schwerdt. Modelling nox-formation in combustion processes. *MSc Theses*, 2006.

[158] C.R. Ferguson and A.T. Kirkpatrick. *Internal combustion engines: applied thermosciences*. John Wiley & Sons, 2015.

[159] F. Centeno, K. Mahkamov, E.E.S. Lora, and R.V. Andrade. Theoretical and experimental investigations of a downdraft biomass gasifier-spark ignition engine power system. *Renewable energy*, 37(1):97–108, 2012.

[160] M.N. Kitanović, P.D. Mra, S.J. Popović, and N.L. Miljić. A thermodynamic work cycle simulation of a syngas-fueled engine. *FME Transactions*, 45(4):572–577, 2017.

[161] J.L. Carrera-Escobedo, C.H. Guzmán-Valdivia, A. Ortiz-Rivera, O. Désiga-Orenday, and M.A. García-Ruiz. Modelo termodinámico de una zona con relaciones para el proceso de combustión en motores alimentados con biogás. *Revista mexicana de ingeniería química*, 12(3):649–660, 2013.

[162] J.L.E. Carrera, J.M.A. Riesco, S.M. Martinez, F.A.C. Sanchez, and A.M. Gallegos. Numerical study on the combustion process of a biogas spark ignition engine. *Thermal Science*, 17(1):241–254, 2013.

[163] B. Gamiño and J. Aguillón. Numerical simulation of syngas combustion with a multi-spark ignition system in a diesel engine adapted to work at the otto cycle. *Fuel*, 89(3):581–591, 2010.

[164] G. Sridhar, P.J. Paul, and H.S. Mukunda. Zero-dimensional modelling of a producer gas-based reciprocating engine. *Proceedings of the Institution of Mechanical Engineers, Part A: Journal of Power and Energy*, 220(8):923–931, 2006.

[165] N. Peters. Four lectures on turbulent combustion. *ERCOFTAC Summer School*, 1997.

[166] E. Fanelli, A. Viggiano, G. Braccio, and V. Magi. On laminar flame speed correlations for h2/co combustion in premixed spark ignition engines. *Applied energy*, 130:166–180, 2014.

[167] F. Zhang, R. Yu, and X. Bai. Detailed numerical simulation of syngas combustion under partially premixed combustion engine conditions. *International Journal of hydrogen energy*, 37(22):17285–17293, 2012.

[168] V. Pessina, A. D'Adamo, C. Iacovano, S. Fontanesi, S. Martinez, and P. Lacava. Numerical simulation of syngas blends combustion in a research single-cylinder engine. Technical report, SAE Technical Paper, 2019.

[169] X. Kan, D. Zhou, W. Yang, X. Zhai, and C. Wang. An investigation on utilization of biogas and syngas produced from biomass waste in premixed spark ignition engine. *Applied energy*, 212:210–222, 2018.

Corresponding Author: vinicio.magi@unibas.it

[170] F.Y. Hagos, A.R.A. Aziz, and S.A. Sulaiman. Syngas (h2/co) in a spark-ignition direct-injection engine. part 1: Combustion, performance and emissions comparison with cng. *International journal of hydrogen energy*, 39(31):17884–17895, 2014.

[171] F.Y. Hagos, A.R.A. Aziz, and S.A. Sulaiman. Effect of injection timing on combustion, performance and emissions of lean-burn syngas (h2/co) in spark-ignition direct-injection engine. *International Journal of Engine Research*, 17(9):921–933, 2016.

[172] F.Y. Hagos, A.R.A. Aziz, and S.A. Sulaiman. Methane enrichment of syngas (h2/co) in a spark-ignition direct-injection engine: Combustion, performance and emissions comparison with syngas and compressed natural gas. *Energy*, 90:2006–2015, 2015.

[173] M. Fiore, A. Viggiano, E. Fanelli, G. Braccio, and V. Magi. Influence of piston shape and injector geometry on combustion and emission characteristics of syngas in direct-injection spark-ignition engine. *Energy Procedia*, 148:392–399, 2018.

Corresponding Author: vinicio.magi@unibas.it